CHAPTER 7

Capacitive Deionization (CDI): An Alternative Cost-Efficient Desalination Technique

Soujit Sen Gupta, Md Rabiul Islam, Thalappil Pradeep

DST Unit of Nanoscience (DST UNS), and Thematic Unit of Excellence (TUE), Department of Chemistry, Indian Institute of Technology Madras, Chennai, India

7.1 Introduction

Availability of clean drinking water is a basic human right, according to the United Nations [1]. There is a shortage in the supply of clean drinking water because of the exponential growth of human population. Due to increased industrialization, agriculture, and climate change, the existing fresh water is also getting contaminated. For meeting the demand of safe drinking water globally, methods such as brackish and seawater desalination were introduced. Multiple water desalination techniques to accomplish this, such as distillation, reverse osmosis (RO), and electrodialysis have emerged successfully in the last few decades. These techniques produce clean water but are either cost or energy-inefficient. Capacitive deionization (CDI) is an emerging desalination technology in the 21st century. CDI has multiple advantages over other desalinating processes: (i) the technique works by the process of electroadsorption, and is even more energy-efficient, as it does not require any high-pressure pumps; (ii) as the module works in 0.8–2.0 V, it can be combined with solar/wind power and can work in remote areas, where availability of electricity is a major issue; (iii) water reject is much less as compared with other techniques such as RO; (iv) carbon particles can withstand much higher temperature than membranes, thereby can be used for wider applications; and (v) as, the device works like a capacitor and high-energy recovery is possible.

Although CDI has multiple advantages over other techniques, the limitation lies on the availability of sustainable electrode materials having high electroadsorption capacity and high average salt adsorption rate (ASAR). An appropriate material for CDI electrode should have the following characteristics: (i) large surface area; (ii) high porosity (both meso and micropores); (iii) high electrical conductivity; (iv) electrochemical stability; (v) bio-inertness; (vi) fast adsorption-desorption kinetics; (vii) good wetting behavior; (viii) low cost; and (ix) scalability.

Advances in Water Purification Techniques. https://doi.org/10.1016/B978-0-12-814790-0.00007-7

Electrodes materials used for CDI are activated carbon, carbon cloth, ordered mesoporous carbon, carbon nanofibers, carbon nanotubes/multiwalled carbon nanotubes (CNTs/MWCNTs), and graphene and graphene-based composites.

A CDI cell comprises of a pair of porous electrodes (especially made of carbon), separated by a nonconducting membrane called a separator. When a potential difference is applied to the electrodes, the electrodes get charged (called as cell voltage or charging voltage). Typically, the cell voltage ranges from 0.8 to 2.0 V. The ions present in the feed water migrate to the electrical double layer (EDL) of the oppositely charged porous carbon electrodes. The ions are electrostatically held at the EDL until an equilibrium is reached when no more ions gets adsorbed. This step is known as electroadsorption and subsequently, desorption happens when the potential is reversed or the external power supply is shorted. During this step, the ions leave the electrodes as the brine stream thereby regenerating them and energy can be recovered from the charge, that is, leaving the cell.

A major problem of CDI lies in the regeneration step. When the electrodes are saturated with oppositely charged ions and reaches an equilibrium, the adsorption step is stopped and the terminals are reversed for desorption. During this step, the adsorbed ions will get desorbed in the bulk fluid but simultaneously the oppositely charged ions from the solution will get adsorbed on the electrodes. Actually, the adsorption and desorption occur at the same time during this step. Therefore, the amount of salt which is adsorbed in the first cycle is not desorbed completely during the desorption step. The residual ions in the electrodes decrease the adsorption efficiency of the material in the next adsorption step. An improvement in the efficiency was shown by the incorporation an ion-exchange (IEX) membrane on top of the porous carbon electrodes and the technique is called membrane capacitive deionization (MCDI) [2]. The membrane can be put in front of the electrodes either as a stand-alone film of 50–200 μm or can be coated on to the electrode surface with a typical thickness of around 20 μm.

In the case of MCDI, the cations penetrate freely through the cation-exchange (CEX) membrane and are held electrostatically in the vicinity of the EDL of the negatively charged electrode, that is, cathode. Similarly, the anions permeate through the anion-exchange (AEX) membrane to the positively charged electrode, that is, anode and get adsorbed. During the regeneration step, when the potential is reversed, the cations from the electrode are desorbed and permeate through the CEX to the bulk fluid, while the presence of CEX will block the anions to penetrate and get adsorbed on the electrode surface even while the electrodes are positively charged. Similarly, in the case of AEX, the cations will not permeate through in the desorption step. Thus, during the regeneration step, no adsorption occurs unlike that of the conventional CDI and all the ions which get adsorbed are desorbed. The next adsorption cycle happens again by reversing the polarity of the power supply, having a fresh electrode surface for adsorption. Thus, there is no loss of adsorption efficiency of the electrodes in the case of MCDI. Schematic in Fig. 7.1 shows the basic mechanism of CDI (Fig. 7.1A) and MCDI (Fig. 7.1B) process [3]. With this concept, Lee et al. in 2006 first developed an MCDI unit for desalinating power plant waste water [4].

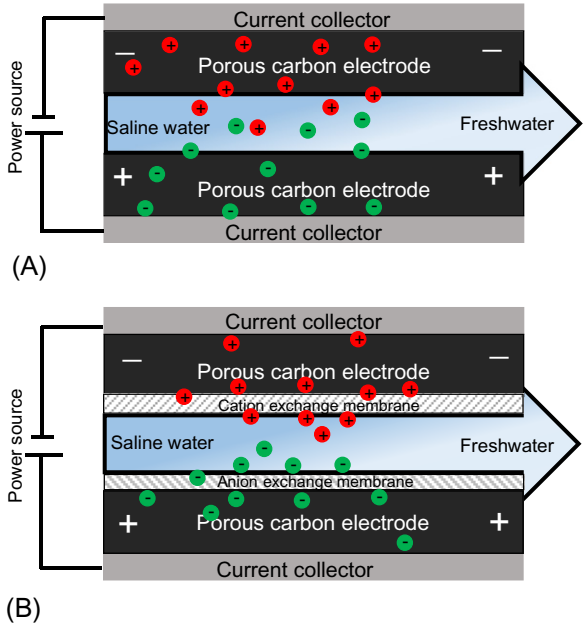

Fig. 7.1

A schematic showing the working principle of (A) capacitive deionization (CDI) and (B) membrane capacitive deionization (MCDI) during the electroadsorption process. *Modified from Porada S, Zhao R, van der Wal A, Presser V, Biesheuvel PM, Review on the science and technology of water desalination by capacitive deionization. Prog. Mater. Sci. 58(8): 1388–1442, 2013.*

They claimed that the salt removal rate was 19% more than of conventional CDI and the salt removal capacity was 92% at an operational potential of 1.2 V using 1000 ppm of NaCl, the energy requirement was 1.96 Wh/L. Długołęck and van der Wal in 2013 showed that the energy recovery for MCDI [5] was 83% as compared with that of 62.1% in case of CDI [6]. They also suggested that by implementing energy recovery as an essential part of the MCDI operation, the overall energy consumption can be as low as 0.26 (kWh)/m^3 of produced water to reduce the salinity by 10 mM and this value is independent of feed water concentration.

In the 21st century, CDI has gone through various modifications than the early work started in the mid-20th century. The modifications include the flow-through electrodes where the water is directed from the top of electrodes, introduction of IEX, constant current operation, salt release at reverse voltage, energy recovery from the desorption cycles, and stop-flow operation during ion release. On the materials point of view, new materials and composites are still emerging in search of novel electrodes having high electroadsorption capacity.

7.2 History of CDI

Historically, the technique of desalination of water using porous "inert" carbon electrodes was reported by Blair and Murphy in the early 1960s and was termed as "electrochemical demineralization of water." In those days, it was assumed that the ions from water were

removed by specific functional chemical groups present on the carbon surface by forming an ionic bond. Evans and Hamilton in 1966 studied the mechanism of demineralization and regeneration at carbon electrodes using Columbic and mass-balance analysis [7]. The efficiency of the salt removal capacity was assumed to be proportional to the concentration of the functional group present on the electrode surfaces. In 1968, Reid designed a 20 gallon/day desalination unit (named as DC-5 demineralization unit, shown in Fig. 7.2) and has shown its commercial relevance [8]. It was tested with natural saline water and the effect of flow rate, pH, cell potential, turbidity, bacteria, algae, and the detoriation of the electrodes were demonstrated. Removal efficiency of various ions like sodium, magnesium, calcium, chloride sulfate, nitrate, and phosphate in the context of drinking water was also mentioned.

The theory of EDL was proposed by Johnson et al. in 1970 as the actual mechanism responsible for reversible electrosorption of salt water using porous carbon electrodes [9]. The work stated that the adsorption capacity of the electrodes depends on the applied potential, available surface area, and the electrical capacity of the double layer. Multiple reports were published by the same group in the next few years but they have to discontinue the study because of the instability of electrodes [10]. A preliminary cost estimation was also presented where it was claimed that a cost-efficient desalination technique by this technology can be achieved only if stable high surface area electrodes are produced.

Electrode material development started from the 1990s, Adelmann used activated carbon electrodes and used as a flow-through capacitor in 1990. The major break-through came by the

Fig. 7.2

The photograph of DC-5, the first 20 gallon/day demineralization unit. *Data from G.W. Reid, A. Stevens, J. Abichandani, F. Townsend, M. Al-Awady, Field Operation of a 20 Gallons Per Day Pilot Plant Unit for Electrochemical Desalination of Brackish Water, U.S. Dept. of the Interior, Washington, DC, 1968.*

pioneering work of Farmer et al. in 1996 [11], where the term CDI was first used. They reported that deionization was performed using carbon aerogel (CA) electrodes and the ions were removed from water by applying electricity. When a potential difference was applied on the electrodes, the ions moved toward the oppositely charged electrodes and get adsorbed electrostatically in EDL formed at the surface of the electrodes. The methods and apparatus for CDI, effect of cell voltage, and regeneration of electrodes using CA electrodes were patented by Joseph Farmer in 1995. Since, then researchers have continuously looked at new and stable materials for CDI. The same group has consecutively published three patents which served as a stepping stone of the CDI technology in recent days [12]. Shiue et al. in 2001 introduced CNT as the electrode material and was first to use nanomaterials in the electrode system [13].

Welgemoed and Schutt in 2005 developed a bench-scale module of CDI unit and evaluated its performance with respect to other membrane technologies [14]. In all 12 pairs of CA electrodes were used having average density and total accessible area of 0.78 g/cm^3 and 2.29 m^2, respectively. The electrodes were having Brunauer-Emmett-Teller (BET) surface area of 600 m^2/g, bulk resistivity of 20 mΩ cm, and specific capacitance of 2 F/cm^2. They have evaluated the cost requirement for treating 800–10,000 mg/L of brackish water to be 0.5–2.25 Wh/gallon for the CDI technology. Other membrane-based technologies such as RO and electrodialysis were found to be 8.5 and 7.7 Wh/gallon, respectively, at the same conditions. In addition, they have claimed that as CA electrodes are chemically resistant oxidizing agents and therefore the lifetime of the electrodes can be extended to 10 years with proper handling.

In 2004, Adelman in a US patent, first introduced "charge barrier flow-through capacitor," popularly known as MCDI in recent days. The technique was used to desalinate waste water by a pilot plant in the work of Lee et al. [4] Theory and physical understanding of MCDI was given by a group of researcher in Wetsus and collaborators in 2010 [15]. Researchers have worked to enhance the maximum adsorption capacity of the electrode material using graphene and its composites, different composite materials such as nanomaterials, metal oxides, CNTs, carbon from biomass, etc., Kim and Choi in 2012 showed that it was possible to remove selective ions from a mixture by modifying the electrode surface and membrane in MCDI [16]. A great advancement in the field of CDI was made with the introduction of carbon flow electrodes which was able to desalinate sea water having total dissolved solids (TDS) of 31 g/L. [17] The use of ionic group derivitized nano-porous carbon electrodes for CDI was demonstrated by Adelman in 2014 as a proof of concept [18]. Different companies and start-ups have come with CDI products both community and domestic units are now in the market. An overview of CDI development and important milestones in the area is depicted in Fig. 7.3.

7.3 Patents in CDI

After a gap of almost two decades, CDI was reborn with the introduction of CA by J.C. Farmer as a stable material for electrodes, in the early 1990s. He showed the method and apparatus for CDI, electrochemical purification, and regeneration of electrodes.

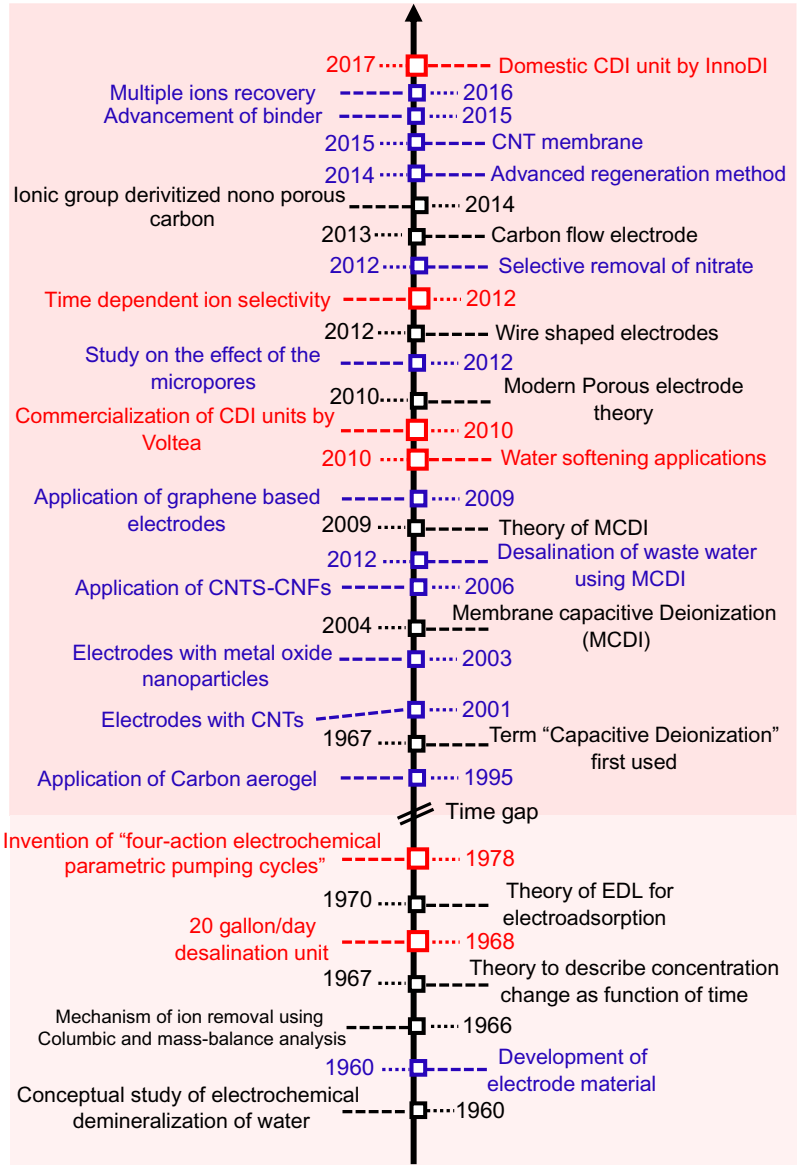

Fig. 7.3

Timeline of developments in CDI indicating the milestones. *Modified from Porada S, Zhao R, van der Wal A, Presser V, Biesheuvel PM, Review on the science and technology of water desalination by capacitive deionization. Prog. Mater. Sci. 58(8): 1388–1442, 2013.*

Eric D. Nyberg gave the idea of electrochemically assisted IEX for efficient CDI. An energy efficient flow-through capacitor, particularly for the concentration and/or separation of seawater was patented by Marc Andelman. He also introduced the concept of charge barrier flow-through capacitor, that is, the use of an IEX. Lih-Ren Shiue in 2002 showed that energy

can be recovered during the regeneration cycle, thereby reduce the overall energy consumption of the system. Ho-Jung Yang in 2009 used transition metals with CNT as an electrode material and introduced an integrated electrode-current collector sheet for CDI. Ali Altaee in the same year showed a process for separating organic compounds from an aqueous medium by using a surfactant. The surfactant reacts with the organic molecules and getting charged, which helps in removing it during the charging cycle. Sean Knapp in the same year showed a method of operating CDI cell using a regeneration cycle to increase pure flow rate and efficiency of the cell. Sundara Ramaprabhu in 2011 shows that ions such as arsenic can be efficiently removed from water using CDI technology. Marc Andelman again in 2012 introduced the concept of polarized electrode for flow-through CDI, where the carbon materials are functionalized and therefore the cells can work efficiently without any IEX. Matthew E. Suss in the same year showed an electrode "flow-through" capacitive desalination system wherein feed water is pumped through the pores of a pair of monolithic porous electrodes separated by an ultrathin nonconducting porous film. The feed water flows through the electrodes and the spacing between electrodes is of the order 10 μm. Kyung-Seok Kang in 2013 has showed that selective ions can be removed from water using MCDI. Patrice Simon used flow electrode architecture for removal of ions from water. Muataz Ali Atieh in 2015 showed that CNT membrane can be used as an electrode for efficient salt removal at low cost. Different binders, composite materials, apparatus, cell architecture, and modified electrodes have been patented in subsequent years. Tae Gong Ryu in 2016 modified the system and showed that ions can be recovered selectively from the system having complex multiions. Table 7.1 shows the list of patents in the course of development of CDI technologies over the years.

7.4 Theory of CDI

The principle of ion removal mechanism in CDI is through physical adsorption on to the surface of the electrodes with the solution and not by oxidation/reduction reaction. It is believed that the Faradic reactions also take place with the carboxy and phenolic group of the electrodes to form a chemical bond with cations in the feed solution. Both these processes contribute to the overall removal efficiency in the CDI cell [53].

In an electrochemical processes when a potential difference is applied to the electrodes, the ions migrate toward the oppositely charged electrodes. This separation mechanism was first studied by Helmholtz in 1893 and described it as EDL model [54]. Similar theory was also given by Perrin in 1904. They assumed that positively charged ions move toward cathode and the negatively charged ions move toward anode creating external Helmholtz layers, leaving a hydrated sheet in the middle consisting of water molecules called the inner Helmholtz layer as shown in Fig. 7.4. This theory has certain limitations as it considered the electrodes to be rigid blocks and neglected the factors like diffusion, mixing, and adsorption of ions on the electrodes

Table 7.1 List of patents in the course of development of CDI technology since, early 1990s

Sl. No.	Inventor (Year of filing)	Patent No.	Title
1	Joseph Farmer (1994) [12a]	US5425858 A	Method and apparatus for capacitive deionization, electrochemical purification, and regeneration of electrodes
2	Joseph Farmer (1995)[12b]	US5954937 A	Method and apparatus for capacitive deionization and electrochemical purification and regeneration of electrodes
3	Eric D. Nyberg (1997) [19]	US5788826 A	Electrochemically assisted ion exchange
4	Tri D. Tran (1999)[12c]	US6309532 B1	Method and apparatus for capacitive deionization and electrochemical purification and regeneration of electrodes
5	Marc D. Andelman (2000) [20]	US6325907 B1	Energy and weight efficient flow-through capacitor, system and method
6	Marc D. Andelman (2001) [21]	WO2002086195 A1	Charge barrier flow-through capacitor
7	Hiroshi Inoue (2002) [22]	US20030189005 A1	Ion exchanger
8	Lih-Ren Shiue (2002) [23]	US6580598 B2	Deionizers with energy recovery
9	Marc Andelman (2004) [2]	US20040174657 A1	Charge barrier flow-through capacitor
10	Ho-Jung Yang (2009) [24]	US20100140096 A1	Electrode for capacitive deionization, capacitive deionization device and electric double-layer capacitor including the electrode
11	Ho-Jung Yang (2009) [25]	US20100181200 A1	Transition metal/carbon nanotube composite and method of preparing the same
12	Ho-Jung Yang (2009) [26]	US8518229 B2	Integrated electrode-current collector sheet for capacitive deionization, capacitive deionization device and electric double-layer capacitor having the same
13	Ali Altaee (2009) [27]	WO2010035004 A1	Capacitive deionization
14	Sean KNAPP (2009) [28]	US20100065511 A1	Method of Regenerating A Capacitive Deionization Cell
15	Kyung-Seok Kang (2010) [29]	US2012032519A1	Capacitive electrode for deionization, and electrolytic cell using same
16	Chang-Hyun Kim (2010) [30]	US20120132519 A1	Capacitive deionization device
17	Kyung Seok Kang (2010) [31]	US20110147212 A1	Ion selective capacitive deionization composite electrode, and method for manufacturing a module
18	Sundara Ramaprabhu (2011) [32]	EP2487278 A2	Methods and systems for separating ions from fluids

Table 7.1 List of patents in the course of development of CDI technology since, early 1990s—Cont'd

Sl. No.	Inventor (Year of filing)	Patent No.	Title
19	David J. Averbeck (2011) [33]	US20120186980 A1	Ion removal using a capacitive deionization system
20	David J. Averbeck (2011) [34]	US9637397 B2	Regeneration of a capacitive deionization system
21	Zhuo Sun (2011) [35]	US9695070 B2	Membrane enhanced deionization capacitor device
22	Marc D. Andelman (2012) [36]	US20130153426 A1	Polarized electrode for flow-through capacitive deionization
23	Matthew E. Suss (2012) [13]	WO2012129532 A1	Flow-through electrode capacitive desalination
24	Moon Il Jung (2012) [37]	S20120273359 A1	Capacitive deionization apparatus
25	Joon Seon JEONG (2013) [38]	US 20130206598 A1	Capacitive deionization apparatus and methods of treating fluid using the same
26	Kyung-Seok Kang (2013) [39]	US20140144779 A1	Method of manufacturing capacitive deionization electrode having ion selectivity and cdi electrode module including the same
27	Antonino ABRAMI (2013) [40]	WO2013183973 A1	Method and plant for the reduction of the concentration of pollutants and/or valuable elements in the water
28	Patrice Simon (2014) [41]	WO2014024110 A1	Method and device to remove ions from an electrolytic media, such as water desalination, using suspension of divided materials in a flow capacitor
29	Myung Dong Cho (2014) [42]	WO 2014195897 A1	Composition for electrode of capacitive deionization apparatus, and electrode including same
30	Yoo Seong Yang (2014) [43]	US5425858 A	Capacitive deionization electrodes, capacitive deionization apparatuses including the same, and production methods thereof
31	Joon Seon Jeong (2014) [44]	US5954937 A	Regeneration methods of capacitive deionization electrodes
32	Yeong Suk Choi (2014) [45]	US5788826 A	Composition for electrode of capacitive deionization apparatus, and electrode including same
33	Zhenxiao Cai (2015) [46]	US6309532 B1	Capacitive deionization system, electrode pack and method for operating the system
34	Muataz Ali Atieh (2015) [47]	US6325907 B1	Fabrication of carbon nanotube membranes

(Continued)

Table 7.1 List of patents in the course of development of CDI technology since, early 1990s—Cont'd

Sl. No.	Inventor (Year of filing)	Patent No.	Title
35	Po-I Liu (2015) [48]	WO2002086195 A1	Binder for capacitive deionization electrode and method for manufacturing the same
36	Yeong suk Choi (2015) [49]	US20030189005 A1	Electrode composition for capacitive deionization device, and electrode for capacitive deionization device containing the same
37	Hyun Sung Choi (2016) [50]	US6580598 B2	Capacitive deionization apparatus
38	Jency DANIEL (2016) [51]	US20040174657 A1	Electrode for capacitive deionization
39	Tae Gong Ryu (2016) [52]	US20100140096 A1	System for recovering multiple kinds of ions

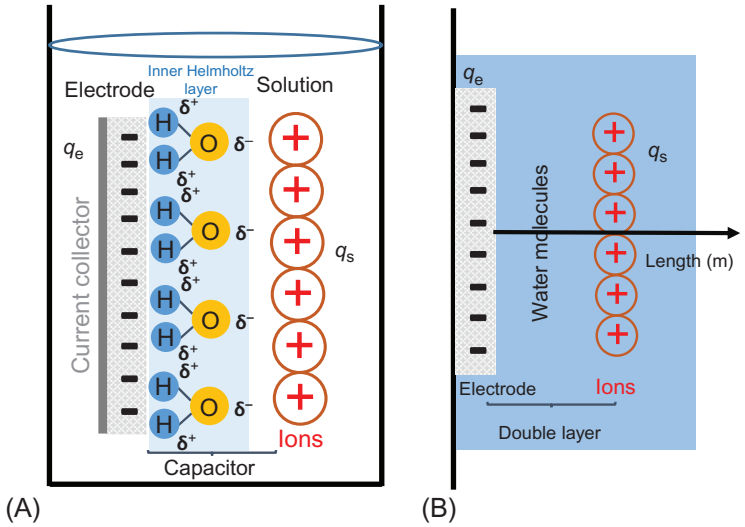

Fig. 7.4

(A) The electrical double-layer (EDL) model of Helmholtz and Parrin and (B) the potential profile with distance across the electrode-solution interface. *Modified from AlMarzooqi FA, Al Ghaferi AA, Saadat I, Hilal N, Application of capacitive deionisation in water desalination: a review. Desalination 342: 2014, 3–15.*

in the solution. The model also suggested that the capacitance does not change with potential and follows the relation:

$$C = \frac{dq}{dV} = \frac{\in \in_0 A}{d} \tag{7.1}$$

Gouy and Chapman in 1913 observed that the electrochemical capacitance strongly depends on the applied potential and the ionic concentration of the feed water. To understand this effect,

they incorporated the parameters of the thermal effect and the gradient of electron density on the double-layer model leading to the so-called diffuse charge model. In this model, the authors applied Maxwell Boltzmann statistics. The charge distribution of the ions in the solution was taken as a function of distance utilizing Thomas Fermi screening distance from the electrodes. The thermal effect was also incorporated in the model using the Boltzmann constant k. The Gouy–Chapman developed a model for capacitance accounting the effect of potential difference φM and temperature T:

$$C = (\cosh(ze_0\varphi M)/2kT)\left(\sqrt{2 \in \in_0 z^2 e_0^2 c_0}/kT\right) \tag{7.2}$$

where z is an integer, e_0 is the ionic cloud charge, φM is the potential difference, k is the Boltzmann constant, T is the temperature of the solution, and c_0 is the ionic concentration in the solution.

The limitation of Gouy–Chapman model arises from the assumption of point charge ions and neglected the ion-ion interaction in the solution, which become significant at higher ionic concentrations. They also assumed that at the interface between the electrode and the bulk solution the dielectric constant is constant. Therefore, the model fails for highly charged diffuse layers. In 1924, Stern combined the Helmholtz–Perrin and Gouy–Chapman models into one as two capacitors in series with the total capacitance expressed as

$$\frac{1}{C} = \frac{1}{C_{\mathrm{H}}} + \frac{1}{C_{\mathrm{G}}} \tag{7.3}$$

where C is the total capacitance and subscripts H and G denote the Helmholtz–Perrin and Gouy–Chapman capacitance, respectively.

Stern's model, is a combination of the Helmholtz–Perrin and Gouy–Chapman model. He proposed that some ions adhere to the electrode in the internal layer as suggested by Helmholtz, giving an internal Stern layer, while some forms a Gouy–Chapman diffuse layer. Close to the electrodes, the Helmholtz–Perrin model dominates, while toward the bulk solution, Gouy–Chapman model dominates. The limitation in Stern's model was that he assumed that there is no interaction of ions and electrodes and therefore, it fails for metallic conductor and in application such as super-capacitors and Li ion battery. But in CDI, the mechanism of ion adsorption follows Stern's model, as the electrodes are inert toward the electrolytes. According to this model, if there are high Stern layer capacities, then it will allow for a high surface charge and, thereby, high salt adsorption capacity (SAC).

7.5 CDI Cell Architectures

The architectures of CDI cells have been a great interest of study in recent years. Two main types of electrode cell architectures are static and flow electrodes. Static electrode architecture includes flow between and flow-through electrodes and membrane CDI. Recent modification in

flow between electrode uses surface-modified anode called inverted CDI (i-CDI) [3]. Flow electrode architecture is feed in where a carbon slurry continuously flows to desalinate feed water [13]. Another new class of CDI architecture is electrostatic ion pumping and desalination through wires. The first and the most used CDI architecture till date is flow between electrodes and is also called flow by electrodes, introduced by Blair and Murphy in the early 1960, later by Oren and Soffer in the 1970s and Farmer et al. in 1996 [12a]. It consists of a pair of porous carbon electrodes, separated by a spacer and the saline water flows perpendicular to the applied potential as shown in Fig. 7.5A. This architecture is commonly used for fundamental studies to determine the maximum salt adsorption capacity (mSAC), to determine the performance of new and novel electrode materials and salt removal at various feed concentrations. Johnson et al. in the 1970s introduced the concept of flow-through electrodes, where the feed water is passed parallel to the applied electric potential and straight through the porous electrodes as shown in Fig. 7.5B. Avraham et al. in 2009 reintroduced the concept after almost 40 years, where they introduced the concept of charge efficiency [55]. Later, the same group compared the charging efficiency between flow-through and flow-between electrodes and claimed for faster cell charging for flow-through electrodes. Suss et al. in 2012 also claimed high efficiency and high rate of adsorption for CA as active electrode in the flow-through architecture [13]. The main advantage of this architecture over the other is the minimization of the spacer thickness from 200–500 μm in flow between to 10 μm in flow-through. As the spacer thickness is reduced, the ionic resistance of the cell is lowered with increased adsorption rate. This architecture requires the electrode material to be porous with both micropores (which enables fast mass transfer) and micropores (which helps in adsorption of ions).

One of the major developments in CDI cell architecture occurs with the introduction of IEX in front of the porous carbon electrodes called MCDI. The concept was first introduced by Andelman in 2004, where he called it as charge barrier flow capacitor [2]. Lee et al. in 2006 demonstrated the MCDI system for desalination of thermal power plant waste water [4], where they used an AEX on top of the anode and CEX on top of the cathode as shown in Fig. 7.5C. They claimed that the efficiency of MCDI was much higher than CDI (flow between) in the contest of salt removal capacity and rate. The membranes can be either placed as a free standing or can be coated over the electrodes. The thickness of the membrane while coating can be thinner and have higher salt removal efficiency with respect to stand-alone membranes [56]. The incorporation of membrane in front of the electrode has two advantages; first, the IEX blocks the co-ions to leave the electrode surface and thereby increases the SAC and second, during the desorption step, it fully flushes the counter-ions and therefore completely regenerated the electrode surface for the next adsorption cycle. In addition to this, membranes can be tuned for selective adsorption of ions having the same charge sign, which thereby, helps in selective removal of ions from a multiion system [16]. The architecture is most widely used in recent days and in the last one decade there have been a tremendous development of MCDI in its theoretical understanding [15, 57], membrane materials and in commercial applications.

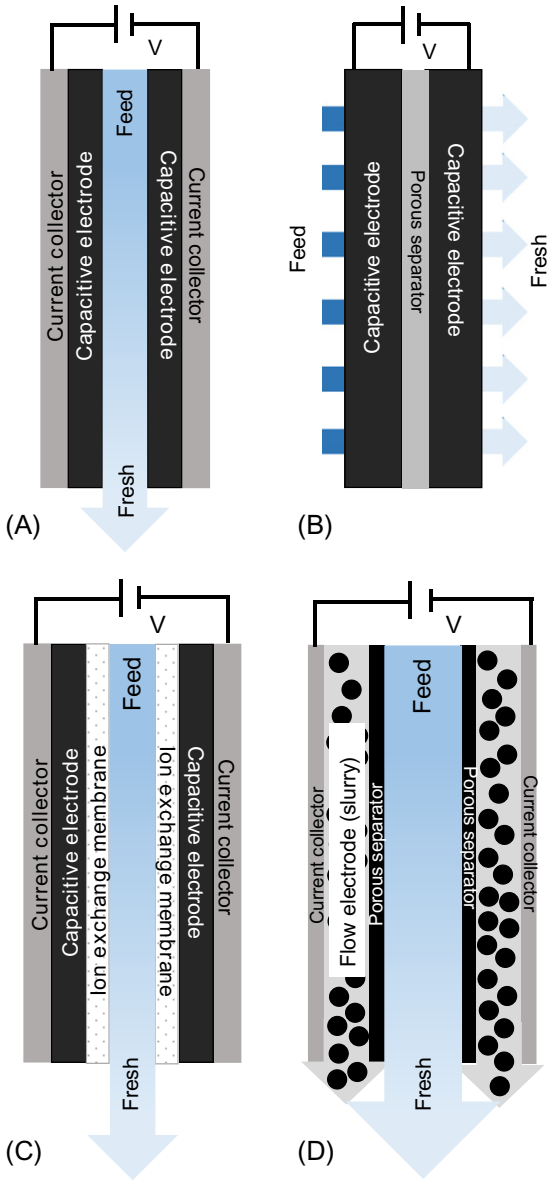

Fig. 7.5
Different cell architectures used for CDI, (A) flow between, (B) flow-through, (C) MCDI, and (D) carbon flow electrodes.

A new class of cell architecture called carbon flow electrode/flow electrode capacitive deionization (FCDI) cell was introduced in 2013 by Jeon et al. [17] In this architecture, carbon slurry is passed through the electrode compartments having opposite charge as shown in Fig. 7.5D. The cations migrate toward the cathode and anions move toward the anode and get

electroadsorbed. The main advantage of this architecture is that the carbon slurry is continuously passed through the compartment and the ions continuously get adsorbed and desorption happens in a different compartment downstream. In the case of static CDI, the ions are adsorbed until the electrodes get saturated and then the terminals have to be reversed to desorb the ions. The steps require complicated fluid handling and loss of efficiency as the adsorption and desorption cycle repeats at regular intervals. Another advantage of FCDI over static CDI is that the former introduces uncharged carbon particles continuously and thereby increases the desalination capacity as the effective capacitance increases. Therefore, FCDI can desalinate water of higher salinity and even sea water having TDS of 31 g/L with an efficiency of 95% and can overcome the limitation of conventional CDI as claimed by Jeon et al.

7.6 CDI Electrode Parameter Metrics

The field of CDI has enormously grown in the last one decade. Therefore, there is a need for the standardization of CDI cell performance. Different parameters which affect the efficiency of the electrodes are the active carbon materials having, porosity, pore size and pore volume, specific surface area, electrical conductivity, specific capacitance, and chemical inertness.

7.6.1 Maximum Salt Adsorption Capacity

In CDI, the most important parameter for defining the performance of a unit is the SAC. Soffer and Folman in 1972 first introduced SAC during a charge-discharge cycle [58]. The adsorption and desorption cycles can have different time duration, ranging from a few minutes, where the adsorption is fast but not complete and they can also be for a few hours where the saturation or equilibrium is reached for complete adsorption. For the latter, one can calculate the mSAC of an electrode, which is better known as equilibrium salt adsorption capacity (eqSAC). To reach the eqSAC, the cell potential and the salt concentration of the feed water should be constant throughout the adsorption cycle. At equilibrium, no more adsorption happens and can be calculated differently for batch mode and single-pass method. In batch mode, the salt removed is calculated by decrease in the salt concentration in the system multiplied with the total volume and is dependent on the initial salt concentration. For the single-pass method, the equilibrium concentration is reached when the input concentration of the feed water equals the output concentration over a time at a constant flow rate. The value of mSAC is calculated by the change in the effluent concentration over a time multiplied by the flow rate, that is, the total volume of water passed to reach the equilibrium. The SAC and mSAC is typically reported by calculating the total salt removal dividing with the total adsorbent weight and expressed in mg/g of the electrodes. Reports have been made either considering the total electrode weight (i.e., the carbon and the binder) or only with the active material (i.e., the porous carbon). Fig. 7.6 shows the maximum adsorption capacity of the electrode materials reported in years.

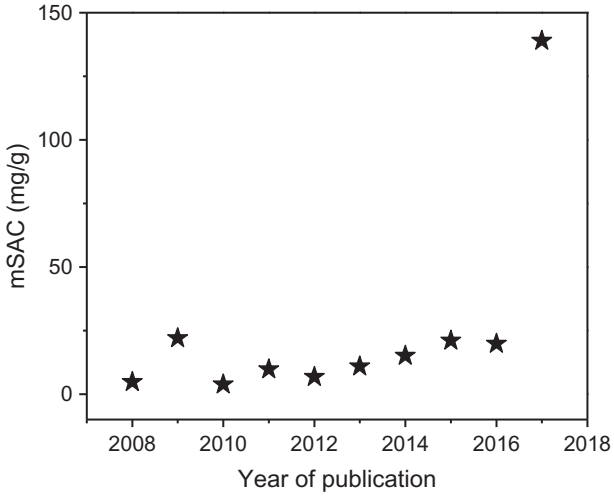

Fig. 7.6
The trend in maximum salt adsorption capacity (mSAC) of different materials over the last decade using different carbon-based electrode materials in batch study, at 500 mg/L of NaCl concentration.

Table 7.2 shows the adsorption capacity of different electrode materials at different concentrations of feed water at different modes of operation. It is important to note that the mSAC is only an electrode property and does not affect by any cell component when all other operational parameters are kept constant. This is an important and mostly used metrics in CDI community to assess the performance (electroadsorption of ions) of electrode material.

7.6.2 Average Salt Adsorption Rate (ASAR)

Another parameter which gives an insight into the performance of CDI cell is ASAR. The value of mSAC gives an indication for the amount of salt adsorbed by the CDI electrode but it gives no information for the adsorption kinetics. ASAR helps us to find the rate at which the salt is adsorbed on the electrodes and it is expressed in mg/g/min. Where, mg is the amount of salt adsorbed, g is the weight of the adsorbent, and min is the average time for the charging or discharging step. Unlike mSAC, ASAR depends on multiple external factors such as flow rate, applied potential, initial feed water concentration, and also the cell architecture. As, for example, if two systems have the same CDI electrode materials and also the thickness of the electrodes are equal then flow-through cell architecture have higher ASAR than flow-by electrode architecture. This is because in the flow-through system, the gap (i.e., the spacer distance) between the electrodes is smaller than that of flow-by system, thus lowering cell resistance and thus cell charging time. For the same electrode and at the same operational potential, ASAR will vary with the flow rate of the feed water. Applied potential plays an important role in deciding the ASAR value, ASAR will increase with the increase in the potential, reaches a maximum, and then decreases. The decrease later is due to the possibility of

Table 7.2 mSAC of different CDI electrode material at different initial salt concentration (mg/L)

Sl. No.	First Author (Year of Publication) [Ref.]	Journal	Materials	Initial Conc. (mg/L)	mSAC (mg/g)
1	J.C. Farmer (1996) [11]	J. Electrochem. Soc.	Carbon Aerogel (CA)	500	2.90
2	K. L. Yang (2001) [59]	Langmuir	CA	1000	2.00
3	K. Dai (2005) [60]	Mater. Lett.	MWCNTs	3000	1.70
4	S. Wang (2007) [61]	Sep. Purif. Technol.	MWCNTs	3500	9.35
5	P. Xu (2008) [62]	Water Res.	CA	2250	7.10
6	H. Li (2009) [63]	J. Mater. Chem.	Graphene	25	1.85
7	H. Li (2010) [64]	Environ. Sci. Technol.	Graphene-like nanoflakes	25	1.35
8	R. Zhao (2010) [65]	J. Phys. Chem. Lett.	Commercial activated carbon electrode	292	10.90
9	C. Tsouris (2011) [66]	Environ. Sci. Technol.	Resorsinol-based mesoporous carbon (MC)	5000	15.20
10	J. Landon (2012) [67]	J. Electrochem. Soc.	Carbon Xerogel	260	3.20
11	H. Wang (2012) [68]	J. Mater. Chem.	Graphene	86.9	0.88
12	Z. Wang (2012) [69]	Desalination	Graphene-CA	65	3.23
13	B. Jia (2012) [70]	Carbon	Sulfonated graphene Ns	250	8.60
14	M. E. Suss (2012) [71]	Energy Environ. Sci.	Microporous carbon aerogel monoliths	5800	10.20
15	D. Zhang (2012) [72]	Nanoscale	Graphene/mesoporous carbon	40	0.73
16	D. Zhang (2012) [73]	J. Mater. Chem.	Graphene/carbon nanotube	29	1.40
17	H. Li (2012) [74]	J. Mater. Chem.	RGO-AC	29	2.94
18	Z. Peng (2012) [75]	J. Mater. Chem.	Ordered mesoporous carbon–CNTs	46	0.63
19	X. Wen (2013) [76]	J. Mater. Chem. A	3D Graphene-based hierarchically porous carbon composites	25	6.18
20	G. Wang (2013) [77]	Sep. Purif. Technol.	Highly mesoporous AC	500	10.90
21	H Yin (2013) [78]	Adv. Mater.	Graphene-Aerogel	500	9.90
22	Z. Y. Yang (2014) [79]	Adv. Funct. Mater.	Sponge-templated graphene	106	4.95
23	Y. Liu (2014) [80]	J. Mater. Chem. A	CNRs	500	15.12
24	A. G. El-Deen (2014) [81]	Desalination	MnO_2-Nanorods@graphene	~50	5.01
25	X. Xu (2015) [82]	Sci. Rep.	Graphene sponge	500	14.90
26	P. Nalenthiran (2015) [83]	ACS Appl. Mater. Interfaces	Cellulose-derived graphenic fibers	500	13.10
27	A. G. El-Deen (2015) [84]	Desalination	RGO/TiO_2	300	9.10

Table 7.2 mSAC of different CDI electrode material at different initial salt concentration (mg/L)—Cont'd

Sl. No.	First Author (Year of Publication) [Ref.]	Journal	Materials	Initial Conc. (mg/L)	mSAC (mg/g)
28	G. Rasines (2015) [85]	Carbon	N-doped CA	1500	8.20
29	Xingtao Xu (2015) [86]	J. Mater. Chem. A	Graphene/CNT	500	18.70
30	R. Kumar (2016) [87]	Carbon	CA	800	10.54
31	A. S. Yasin (2016) [88]	Sep. Purif. Technol.	Graphene oxide/ZrO_2	~50	4.55
32	H. Zhang (2016) [89]	RSC Adv.	Moderately oxidized graphene-CNT	500	8.45
33	S. Zhao (2016) [90]	Applied Surface Sci.	N-Doped porous hollow carbon spheres	500	12.95
34	W. Kong (2016) [91]	Nano Res.	Holey graphene hydrogel	5000	26.80
35	X. Xu (2016) [92]	J. Mater. Chem. A	hCNT/PCP	2000	20.50
36	T. Gao (2017) [93]	Desalination	Mesoporous carbons	250	4.80
37	D. Xu (2017) [94]	ACS Sustain. Chem. Eng.	N, P codoped meso-/microporous carbon	1000	20.78
38	S. Zhao (2017) [95]	RSC Adv.	micro/mesoporous carbon sheets	500	17.38
39	H. Wang (2017) [96]	ACS Sustain. Chem. Eng.	N-doped hollow multiyolk@shell carbon (HMYSC)	500	16.10
40	T. Wu (2017) [97]	Environ. Sci. Technol.	Porous carbon nanosheets (PCNSs)	500	15.60

Data after 1996 are given.

electrolysis above a certain potential for the electrode material. So, there is an optimum value where the ASAR is maximum. Also, the CDI electrode material can affect the value of measured ASAR, as for example, if the electrodes have larger mesopores than micropores, which allows higher salt sorption then the ASAR will be higher. Thus, ASAR is a combination of several factors and therefore it should be considered a cell component property rather than only electrode property.

7.6.3 Charge Storage Capacity

Along with mSAC and ASAR, the third metrics for CDI cell are the charge storage capacity, this metric is of a great importance in the super-capacitor community. This metric/parameter is obtained from the amount of current used vs. time during the charging and discharging cycles. Data for current are expressed in units of Amperes (A = C/s), and it is integrated with respect to time to obtain the electric charge transfer between two oppositely charged electrodes of the cell

(in units of Coulombs, C). For obtaining the capacitance of a single electrode, the capacitive charge (i.e., C) is divided by the mass of a single electrode material and by half of the cell voltage (assuming cell symmetry), called as specific capacitance.

7.6.4 Charge Efficiency

The electric charge accumulates on the electrodes during the adsorption cycle (i.e., charging) and is released during desorption cycle (i.e., discharging). To express the charge in moles, the accumulated electric charge is divided with Faraday ($F = 96{,}485$ C/mol) and is a measure of salt adsorption per cycle. Thus, charge efficiency can be defined as the ratio of adsorbed salt over charge. Avraham in 2009 [55] first used the term "charge efficiency" and Zhao et al. in 2009 [65] used the symbol Λ while describing charge efficiency. Λ depends on cell potential and feed water salt concentration. Generally, Λ increases when the charging voltage increases and decreases with decreasing salt concentration as shown in Fig. 7.7.

Λ is an important parameter for evaluating the performance of the CDI cell. First, the energy requirement can be accounted from the value of Λ, a higher Λ means lower energy consumption. Zhao et al. in 2012 provided experimental data to compare the energy consumption in MCDI and CDI at constant voltage and constant current operation [57a]. For a constant charging voltage, MCDI has higher charge efficiency and therefore, consume lower energy than CDI. Second, during charging when the equilibrium is reached, equilibrium EDL theory can predict Λ, or vice versa [57a].

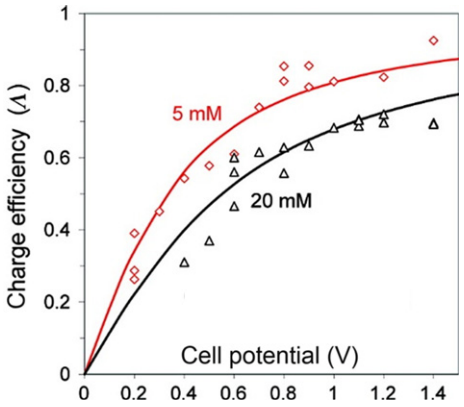

Fig. 7.7

Variation of charge efficiency Λ as a function of cell potential and feed water concentrations of 5 and 20 mM. *Reproduced with permission from Zhao R, Biesheuvel PM, Miedema H, Bruning H, van der Wal A, Charge efficiency: a functional tool to probe the double-layer structure inside of porous electrodes and application in the modeling of capacitive deionization. J. Phys. Chem. Lett. 1(1): 2010, 205–210.*

7.6.5 Porosity

Porosity is regarded as one of the most important factors for electrochemical capacitors and CDI electrodes. The efficiency of CDI electrodes, that is, the capacitance depends on the accessible pores and the pore sizes. According to the IUPAC, pores are classified into three types: macropores (>50 nm), mesopores (2–50 mn), and micropores (<2 nm) [98]. Some reports suggest that the pore size less than 0.5 nm [99] is not accessible for ion adsorption as the ions are in hydrated form in aqueous solutions. As per solvated ion adsorption theory, high energy of the order of kilojoules per mole is required to remove the hydrated shell [100]. Therefore, it was believed that a bimodal porosity containing both micro and mesopores is required in carbon material for enhanced capacitance and ion adsorption. Ion adsorption occurs in the micropores whereas the mesopores allows fast mass transport of electrolyte to the micropores. Depending upon the pore distribution, Hwang et al. proposed a theory of splitting of the capacitance in two different regimes of pores. For mesopores, a traditional EDL model was followed:

$$\frac{C}{A} = (\in_r \in_0) / \left(b^* \ln \left(\frac{b}{b-d} \right) \right) \tag{7.4}$$

where C is the capacitance, A is the specific surface area, b is the pore radius, and d is the distance of approach of the ions to the carbon electrodes. For micropores, it was assumed that the ions enter the pores gets desolvated and stack as a line, where cylindrical electrical wire model was followed:

$$\frac{C}{A} = \in_r \in_0 / b^* \ln \left(\frac{b}{a_0} \right) \tag{7.5}$$

where a_0 is the desolvated ion size.

7.7 Emerging CDI Electrode Materials

7.7.1 Activated Carbon

The most widely used material for CDI since the early 1970s is alternating current (AC). It is generally derived from raw materials such as petroleum, coconut shell, wood, rice husk, etc., having a surface area of 500–2300 m^2/g, with tunable porosity and varying hardness [101]. Zou et al. in 2008 claimed that electrosorption capacity of activated carbon can be enhanced by chemical surface modification or by incorporating metal-oxide nanoparticles such as TiO_2 [102]. Zeng et al. in 2017 reported that the electroadsorption capacity of commercially available AC can be increased 5.09 times by plasma treatment [using coupled plasma of Ar and 10% O_2, at a pressure of 4.0 Torr, resorsinol-formaldehyde (RF) power ranges from 50 to 100 W for 10 min] [103]. Lado et al. in 2017 reported an abundant, low cost biowaste carbon material (Sugar Cane Bagasse Fly Ash) which after activation with KOH at 800°C, gave high

electrosorption capacity of 48%–74%. They claimed that the presence of small amounts of ether/alcohol functional groups increase the carbon hydrophilicity and hence, increase the SAC [104]. Alencherrya et al. in 2017 showed that the addition of silver and CNTs in AC enhances the electrical conductivity as well as the hydrophilicity, which in terms increase the electrosorption capacity by around twofolds [105]. Chen et al. in 2018 economically prepared ACs recycled from bitter-tea and palm shell wastes and was used for CDI electrodes and showed removal capacity up to 40% using 1000 ppm NaCl solution. They have modified the electrodes with Ag@C core shell nanoparticles to provide additional disinfection ability during desalination [106]. Yashin et al. in 2018 used N_2 and TiO_2/ZrO_2 as a support for AC for enhancing the electrochemical performance [107].

7.7.2 Ordered Mesoporous Carbon

Zou et al. [108] in 2008 had prepared ordered mesoporous composite (OMC) and claimed that the CDI performance was better than AC. The pore size of the OMC material was found to be ~3.3 nm which allows the salt ions to pass through the pores freely and the ordered mesostructure allows fast adsorption and desorption of Na^+ and Cl^- ions. Li et al. in 2009 also found that the CDI efficiency of OMC doped with Ni salt is higher than that of AC. Transmission electron microscopy (TEM) image of OMC is shown in Fig. 7.8A [109]. In case of AC, some surfaces are unavailable for electroadsorption as the micropores are smaller than the hydrated radii of the ions. Tsouris et al. in 2011 prepared self-assembled mesoporous carbon

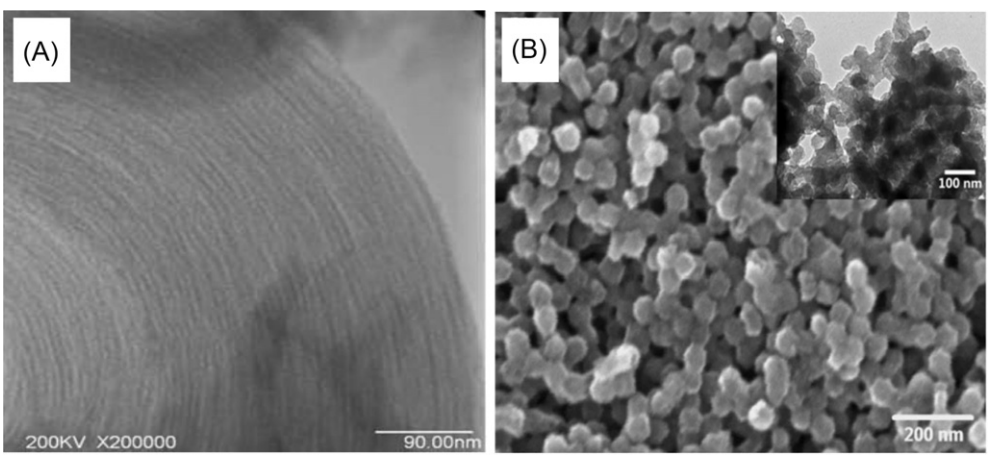

Fig. 7.8

(A) Transmission electron microscopy (TEM) image of ordered mesoporous composite (OMC) [109] and (B) scanning electron microscopy (SEM) image of MCs and the inset shows a TEM image of the same material [93]. *Reproduced with permission from Gao T, Li H, Zhou F, Gao M, Liang S, Luo M, Mesoporous carbon derived from ZIF-8 for high efficient electrosorption. Desalination 108, 2017; Li L, Zou L, Song H, Morris G, Ordered mesoporous carbons synthesized by a modified sol–gel process for electrosorptive removal of sodium chloride. Carbon 47(3): 2009, 775–781.*

using phenolic resins, such as resorcinol or phloroglucinol by sol-gel technique and then carbonization at 750°C [66]. They claimed that the performance of MC was superior to that of CA due to the fact that most of the pores in CA are micropores in the range of 10 Å which are not accessible for the adsorption of ions. Peng et al. in 2012 prepared OMC/CNT composites by the organic-inorganic self-assembly route. With a loading of 10% CNT, the material showed superior electroadsorption capacity and exhibits low energy consumption when compared with pristine OMC for CDI [75]. Wang et al. in 2013 had taken mesoporous activated carbon for CDI and showed that the electroadsorption capacity of the electrodes depended on the solution temperature. The capacity decreased with the increase in temperature [77]. Gao et al. in 2017 prepared MCs by direct carbonization of ZIF-8 at 1000°C in Ar/H_2 atmosphere. They got an adsorption capacity of 4.8 mg/g using 250 mg/L of NaCl solution but claimed that the theoretical mSAC can reach 17 mg/g according to the Langmuir adsorption isotherm. The scanning electron microscopy (SEM) image of MC is shown in Fig. 7.8B and the inset shows a TEM image [93].

7.7.3 Carbon Aerogel (CA)

The revolution of CDI electrodes came with the new class of carbon material called CAs in 1996 by Farmer et al. [11] Traditionally, inorganic aerogels were prepared by hydrolysis and condensation of metal-alkoxides using sol-gel technique. Similar procedure was extended to form organic aerogels and xerogels using resorsinol (R) and formaldehyde (F)/melanin and formaldehyde to form cross-linked gels. These gels were dried and pyrolyzed in inert atmosphere at a temperature of 800–1500°C to form CA [110]. CA has high surface area (400–2600 m^2/g), high electrical conductivity (~25–100 S/cm), high electrochemical stability in water and tunable porosity (the ratio of micro and mesopores).

Yang et al. in 2001 prepared CA electrodes and developed EDL model to predict the electroadsorption of ions. The adsorption largely depends on the pore size of the material. The smaller pores, that is, the micropores do not contribute to adsorption. As the feed water ion concentration increases, the cut-off pore width decreases The cut-off pore width is found to decrease with increasing feed ion concentration and applied potential [59]. Jung et al. in 2007 prepared RF organic aerogel in a cost-effective route using acetone as a solvent exchanger and used ambient drying conditions. The solid was pyrolyzed after drying in N_2 atmosphere at 800°C. They have reported the material having high surface area of 610 m^2/g, very high specific capacitance of 220 F/g, high electrical conductivity of 13.2 S/cm, high porosity of 80%, and low bulk density of 0.5 g/cm^3. They have tested the CA electrodes at 50 mg/L NaCl solution at a flow rate of 400 mL/min at an applied potential difference of 1.5–1.7 V and claimed the removal efficiency was 92.8% and 97.6% at 1.5–1.7 V, respectively [111]. Xu et al. in 2008 had taken CA electrodes and showed the selectivity of I^- is more in the presence of other ions like Br^-, Cl^-, etc. Therefore, they claimed that the technology can be used for iodine recovery from waste water [62].

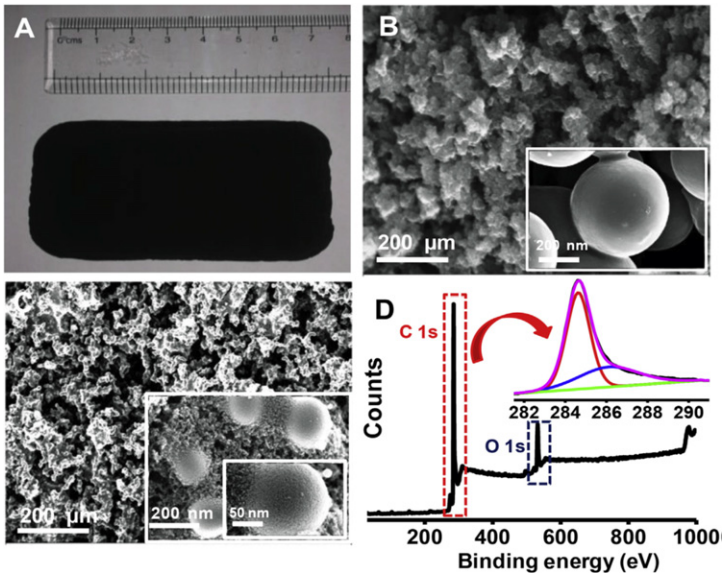

Fig. 7.9

(A) The photograph shows the as-prepared carbon aerogel (CA) block of dimension 7 cm (length) × 3 cm (width) × 1 cm (thick), field emission scanning electron microscopy (FESEM) images of (B) Si-CA and (C) CA, and (D) X-ray photoelectron spectroscopy (XPS) spectrum of CA showing the presence of carbon and oxygen. *Reproduced with permission from Kumar R, Gupta SS, Katiyar S, Raman VK, Varigala SK, Pradeep T., Sharma A, Carbon aerogels through organo-inorganic co-assembly and their application in water desalination by capacitive deionization. Carbon 99: 2016, 375–383.*

Rasines et al. in 2015 prepared N-doped CA polycondensation of resorcinol-formaldehyde-melamine mixtures [85]. Kumar et al. in 2016 prepared Si-CA using RF and tetraethyl orthosilicate (TEOS) as silica precursors. They dried the gel in ambient condition and carbonized it in inert atmosphere at 900°C. The carbonized product formed was Si-CA. CA was prepared subsequently by etching Si with 1 M KOH. Etching of Si enhances the porosity of the composites. Both Si-CA and CA were tested as CDI electrode materials and they showed high efficiency for salt removal with good regeneration property [87]. Spectroscopic and microscopic characterization data of the material are shown in Fig. 7.9.

7.7.4 Other Carbon Derivatives

Poroda et al. in 2012 reported porous carbide-derived carbon material with tunable pore sizes as efficient CDI electrodes. The work emphasized that the adsorption capacity of any carbon material has a positive correlation with subnanometer pores (pore size less than 1 nm) [112]. Liu et al. in 2014 prepared carbon nanorods (CNRs) from nanocrystalline cellulose by heating at 1200°C under inert atmosphere [80]. TEM image of CNR is shown in Fig. 7.10A. CNRs shows high specific capacitance of 264.19 F/g, surface area of 864.10 m^2/g and pore volume of

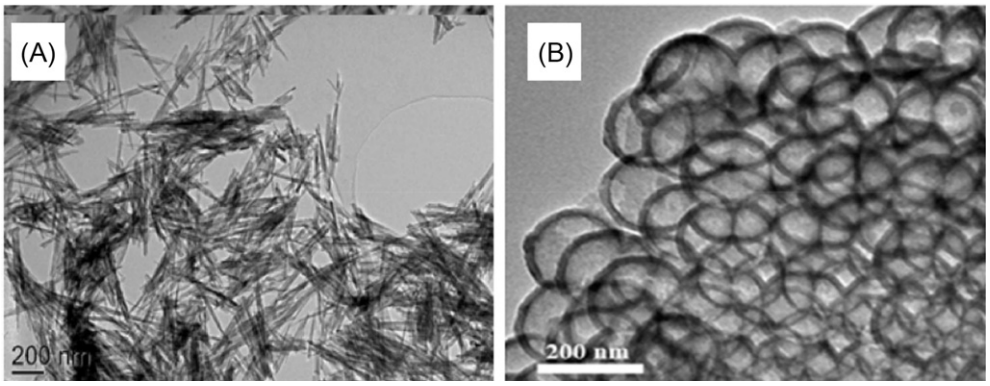

Fig. 7.10

TEM image of (A) carbon nano rods [80] and (B) N-doped hollow carbon spheres [90]. *Reproduced with permission from Liu Y, Pan L, Xu X, Lu T, Sun Z, Chua DH, Carbon nanorods derived from natural based nanocrystalline cellulose for highly efficient capacitive deionization. J. Mater. Chem. A 2(48): 2014, 20966–20972; Zhao S, Yan T, Wang H, Chen G, Huang L, Zhang J, Shi L, Zhang D, High capacity and high rate capability of nitrogen-doped porous hollow carbon spheres for capacitive deionization. Appl. Surf. Sci. 369: 2016, 460–469.*

0.47 cm^3/g. The material shows high adsorption capacity of 15.12 mg/g due to large surface area and low charge transfer resistance. Zhao et al. prepared N-doped hollow carbon spheres as shown in TEM image in Fig. 7.10B. They used polystyrene (PS) spheres as hard templates and dopamine hydrochloride as carbon and nitrogen sources [90]. Recently, sustainable materials derived from biomass are of great interest because of low cost and abundance. The same group in 2017 prepared micro/mesoporous carbon sheets using watermelon peel as a carbon source [95], Wu et al. prepared porous carbon nanosheets using starch [97] and Xu et al. developed N and P co-doped carbon material from biomass with high specific surface area of 2726 m^2/g and 52% of mesopores [94].

7.7.5 Carbon Nanotubes (CNTs)

CNTs are a class of one-dimensional (1D) tubular carbon materials formed by rolling of graphene sheets. They are classified into single-walled carbon nanotubes (SWCNTs) and MWCNTs as per the number of layers. SWCNTs are formed by a single-layer graphene and MWCTs are formed by multilayer graphitic carbon. CNTs can be metallic or semiconducting depending on how the sheets are rolled, which results in armchair, ziz-zag, and chiral configuration [113]. The advantages of CNTs over other carbon materials are that they can carry high current density through the tubes without electronic scattering, that is, the charge transport occurs ballistically [113].

Yan et al. in 2012 prepared SWCNT and polyalinine (PANI) composites by in situ polymerization. The TEM images in Fig. 7.11A and B show that PANI forms a shell around SWCNT. The addition of PANI in SWCNT decreases the specific surface area due to the

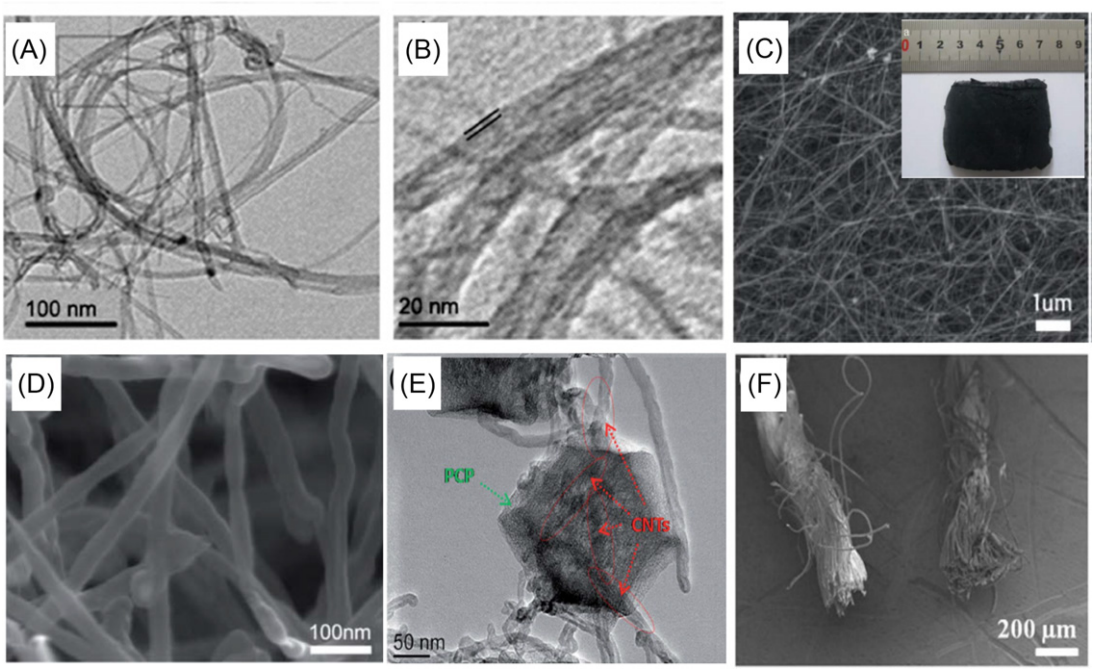

Fig. 7.11

Microscopic characteristics of different carbon nanotube (CNT) composites. (A and B) TEM image of polyalinine (PANI)@CNT composite, PANI forms a shell over single-walled carbon nanotubes (SWCNTs) as shown in (B) [114]. (C) SEM image of CNT sponge [115], the inset shows a photograph of the same. (D) High-resolution scanning electron microscopy (HRSEM) image of CNT sponge showing network-like structure [115]. (E) HRTEM image of hierarchical porous CNT (hCNT)/porous carbon polyhedra (PCP) [92], both CNT and PCP are marked in the figure and (F) SEM image of pristine and CNT threads [116]. *Reproduced with permission from Xu X, Wang M, Liu Y, Lu T, Pan L, Metal–organic framework-engaged formation of a hierarchical hybrid with carbon nanotube inserted porous carbon polyhedra for highly efficient capacitive deionization. J. Mater. Chem. A 4(15): 5467–5473, 2016. Yan C, Zou L, Short R, Single-walled carbon nanotubes and polyaniline composites for capacitive deionization. Desalination 290: 125–129, 2012. Wang L, Wang M, Huang Z-H, Cui T, Gui X, Kang F, Wang K, Wu D, Capacitive deionization of NaCl solutions using carbon nanotube sponge electrodes. J. Mater. Chem. 21(45): 2011, 18295–18299; Moronshing M, Subramaniam C, Scalable approach to highly efficient and rapid capacitive deionization with CNT-thread as electrodes. ACS Appl. Mater. Interfaces 9(46): 39907–39915, 2017.*

removal of micropores but the mesopore volume increases appreciably, which in contrast increases the salt removal efficiency by 12% as compared with SWCNTs. They claimed that the improvement in the adsorption capacity is due to the pi-pi conjugation of the benzenoid chain of PANI and aromatic carbon skeleton of SWCNT [114]. Wang et al. in 2013 prepared CNT sponge electrodes by a chemical vapor deposition (CVD) process using 1,2 dichlorobenzene as carbon precursor and ferrocene as catalyst [115]. CDI cells were prepared using these CNT sponges without any use of binder. Fig. 7.11C shows the SEM image of CNT sponges.

High-resolution scanning electron microscopy (HRSEM) image in Fig. 7.11D shows continuous three-dimensional (3D) web structure and are randomly cross-linked with each other having 20–40 nm in diameter. The inset in Fig. 7.11C shows the photograph of a CNT sponge. They claimed the desalination capacity of the material to be 40 mg/g of electrodes, which was highest at that time.

Xu et al. prepared hierarchical porous CNT/porous carbon polyhedra (PCP) (hCNT/PCP) which is shown in Fig. 7.11E. Hybrid with CNTs and ZIF-8 showed that the material is a good candidate for effective CDI electrodes [92]. Moronshing et al. in 2017 had prepared CDI electrodes using CNT threads having specific surface area of 900 m^2/g, electrical conductivity of 25 S/cm, specific capacitance of 27.2 F/g, and porosity of 0.7 and 3.0 nm with a hydrophilicity having contact angle of 25°. In a flow-through experiment using a single pair of electrodes, having the saline concentration of 50–1000 ppm, they have reported the highest electroadsorption capacity of 139 mg/g for the electrode [116]. SEM image of pristine thread (left) and CNT thread (right) is shown in Fig. 7.11F.

7.7.6 Graphene and Graphene-Based Composites

Since the discovery of graphene by Geim and Novoselev in 2004 [117], it has become subject of major interest. The one atom thick two-dimensional (2D) material with extraordinary electronic, thermal, and electrical properties made the material to be called as a "wonder" material. Graphene and its analogs due to its large surface area, high electrical conductivity, antibacterial property, and tuneable functionalization make the material a potential candidate in water purification applications. Overwhelming number of articles is published in the last decade using graphene as an adsorbent for water remediation.

Li et al. in 2010 first used graphene nano-flakes (GNFs) as a CDI electrode material and showed the electroadsorption capacity was better than that of AC. GNFs were prepared by modified Hummers' method followed by reduction with hydrazine. They conducted CDI experiment with different cations and reported that the higher valence ions with smaller hydrated radii will be strongly adsorbed. The cations with same charge with smaller hydrated radii will be removed preferentially. They concluded that the electroadsorption capacity is in order $Fe^{3+} > Ca^{2+} > Mg^{2+} > Na^{+}$ [118]. Till then many groups have worked with graphene and its composites for making novel and efficient electrode materials. Jia et al. in 2012 prepared graphene nanosheet (GN) from graphene oxide (GO) by a multistep process and used it as an electrode material for CDI. The TEM image of GNs is shown in Fig. 7.12A. The material has mean pore size of 3.3 nm, surface area of 464 m^2/g, and specific capacitance of 149.8 F/g, the GNs electrodes show NaCl removal efficiency of 83.4% and electroadsorption capacity of 8.6 mg/g of electrode material [70]. Yin et al. in 2013 reported highly efficient CDI electrode materials using 3D graphene/metal oxide hybrid composites for the first time [78]. Wang et al. in same year prepared 3D macroporous graphene architecture (3DMGA), which shows high specific surface

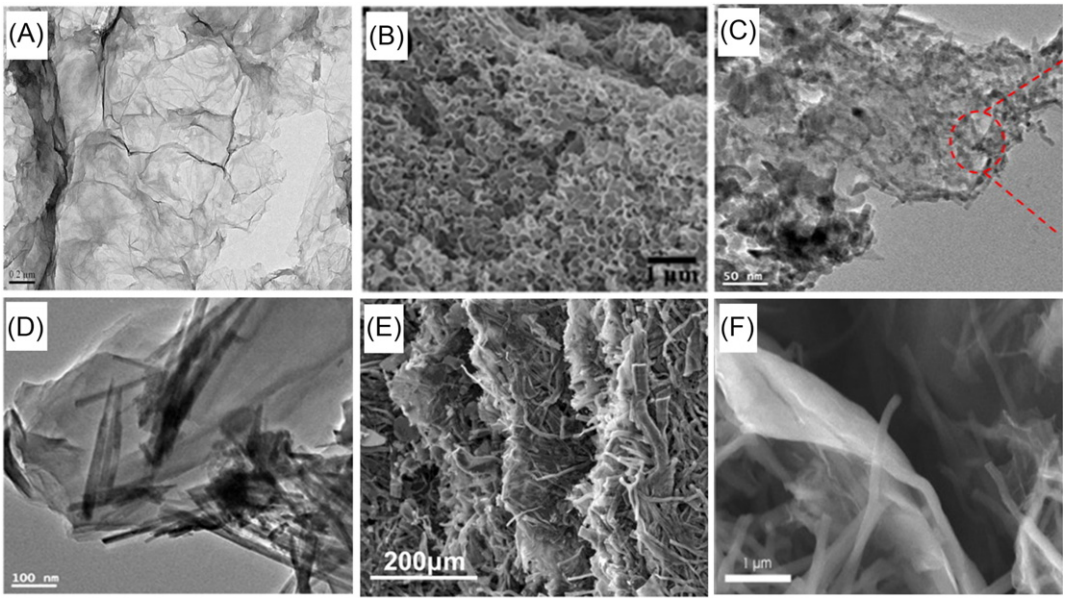

Fig. 7.12

Microscopic images of graphenic materials used for CDI electrodes: (A) TEM image graphene nanosheets (GNs) [70], (B) SEM image of three-dimensional (3D) macroporous graphene architecture [119], TEM images of (C) graphene@MnO_2 nanoparticles and (D) graphene@MnO_2 nanorods [81], (E) SEM image of cellulose-derived graphenic fibers [83], and (F) 3D composite of graphene@carbon fibers [120]. *Reproduced with permission from Jia B, Zou L, Graphene nanosheets reduced by a multi-step process as high-performance electrode material for capacitive deionisation. Carbon 50(6):2315–2321, 2012; El-Deen AG, Barakat NAM, Kim HY, Graphene wrapped MnO2-nanostructures as effective and stable electrode materials for capacitive deionization desalination technology. Desalination 344:289–298, 2014; Pugazhenthiran N, Sen Gupta S, Prabhath A, Manikandan M, Swathy JR, Raman VK, Pradeep T, Cellulose derived graphenic fibers for capacitive desalination of brackish water. ACS Appl. Mater. Interfaces 7(36): 20156–20163, 2015. Luo G, Wang Y, Gao L, Zhang D, Lin T, Graphene bonded carbon nanofiber aerogels with high capacitive deionization capability. Electrochim. Acta; Li H, Liang S, Li J, He L, The capacitive deionization behaviour of a carbon nanotube and reduced graphene oxide composite. J. Mater. Chem. A 1(21): 6335–6341, 2013.*

area and porosity for rapid ion and electron transport when used as CDI electrodes [119]. They prepared 3DMGA by mixing GO and PS, where PS was used as a sacrificial template, which was further dried and calcinized at elevated temperature in an inert atmosphere. The SEM image in Fig. 7.12B shows 3D nature of 3DMGA. Earlier the same group used pyridine to prepare graphene by thermal heating and showed its application in CDI electrodes [68].

El-Deen et al. in 2014 showed that the electroadsorption capacity of graphene increases when MnO_2 nanostructure was incorporate in it. Graphene-wrapped MnO_2 nanostructure was prepared by oxidation-reduction reaction using graphite and manganese sulfate as precursors. The oxidation graphite was done with ammonium peroxysulfate and hydrogen peroxide in the

presence of $MnSO_4$ followed by reduction with piperidine under microwave irradiation. The morphology of graphene MnO_2 nanostructure can be controlled by varying the microwave irradiation time from 15 to 30 min to form graphene@MnO_2 nanorods and graphene@MnO_2 nanorods, respectively, as shown in TEM images in Fig. 7.12C and D [81]. Pugazhenthiran et al. in 2015 prepared cellulose-derived graphenic fibers using tissue paper. Tissue paper was taken along with graphite powder as a conducting agent and TEOS as a silica precursor and the mixture was pyrolyzed under N_2 atmosphere at 700°C. Silica was then etched with aqueous KOH solution to enhance the porosity, especially the micropores in the carbon structure. The SEM image of graphite-reinforced carbon (GrC) is shown in Fig. 7.12E, fiber kind of nature of the material can be seen from the image. The as-prepared material was termed as GrC and was used as CDI electrodes without any kind of binder in a batch mode. GrC showed high electroadsorption property of 13.1 mg/g for 500 mg/L of NaCl solution with an excellent recyclability [83]. Hierarchical hole-enhanced 3D graphene assembly was prepared by Li et al. in 2017 [121] and showed the desalinating capacity of 8.0, 16.9, and 29.6 mg/g in aqueous NaCl concentrations of 80, 270, and 572 mg/L, respectively, at 2.0 V. Luo et al. in 2017 prepared a fascinating 3D porous structure consisting of 1D (i.e., nanofibers) and 2D (i.e., graphene) carbon nanomaterials as shown in Fig. 7.12F [120]. The composite was prepared by carbonization of electrospun polyacrylonitrile with GO sheets. The material showed an adsorption capacity of 15.7 mg/g in 500 mg/L NaCl solution and an electrochemical stability for 100 cycles.

7.8 Electrochemical Impedance Spectroscopy for CDI Electrodes

Impedance is the measure of the ability of a circuit to resist the flow of electrical current. The term impedance refers to the frequency dependence to current flow in a circuit. It assumes an AC of specific frequency in Hz. It can be expressed as

$$Z_\omega = \frac{E_\omega}{I_\omega} \tag{7.6}$$

where, Z_ω is the impedance, E_ω is the frequency-dependant potential, and I_ω is the frequency dependant current.

Electrochemical impedance spectroscopy (EIS)/equivalent series resistance (ESR) is a great technique that uses a small amplitude AC signal to measure the impedance characteristics of electrodes or a cell. To measure the impedance spectrum of an electrochemical cell under test, the AC signal is scanned over a wide range of frequencies. EIS allows the study of capacitive, diffusion, and inductive processes which takes place in the electrochemical cell and even the electron transfer rate of a reaction unlike that of direct current (DC) techniques. EIS has multiple applications which includes in the area of coatings, batteries, fuel cells, photovoltaic, sensors, and biochemistry.

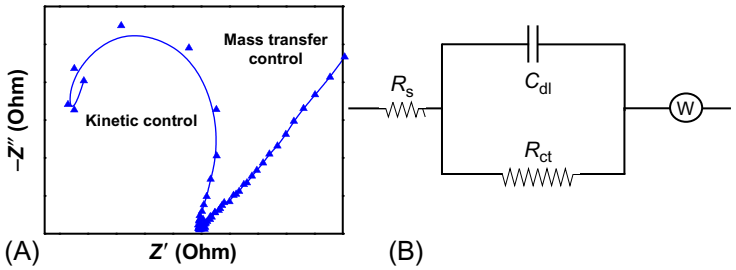

Fig. 7.13

(A) Nyquist plot of graphenic material prepared from cellulose and (B) the equivalent electrical circuit extracted from the plot in part (A). Unpublished data from the authors' laboratory.

EIS data can be represented as a complex plane (Nyquist) plot. Nyquist plot is defined as the "representation of the vector response of a feedback system (especially an amplifier) as a complex graphical plot showing the relationship between feedback and gain." Nyquist plot is generally used for assessing the stability of the system with feedback. In the Cartesian coordinates, the real part is plotted in the X-axis (Z') and the imaginary part is plotted on the Y-axis ($-Z''$).

A Nyquist plot for a graphenic material prepared from cellulose is shown in Fig. 7.13A. The Nyquist curve has two parts (i) head part (semicircle part) and (ii) tail (inclined line). A semicircle at high frequency and an inclined line at low frequency were found here.

Meng et al. [122] explained that from Nyquist plot we can know about the equivalent circuit of the electrodes as shown in Fig. 7.13B, where, R_s is the ohmic resistance, R_{ct} is the electrochemical charge transfer resistance, C_{dl} is the electrochemical double-layer capacitance, and W is the Warburg impedance. C_{dl} of the electrodes is given as follows:

$$C_{dl} = 1/T(j\omega)^{\varphi} \tag{7.7}$$

$$T = C_{dl}^{\varphi}\left(R_s^{-1} + R_{ct}^{-1}\right)^{1-\varphi} \tag{7.8}$$

where ω is the angular frequency (in rad/s) of the AC voltage and φ is the depression angle 90 $(1-\varphi)$ of the semicircle. T is a constant associated with the double-layer capacitance.

In the high-frequency region, the semicircle refers to the polarization resistance which includes the charge-transfer resistance between the electrodes and the salt solution interface. Wang et al. [123] in 2013 in the case of 3DMGAs electrode found a semicircle with small diameter which indicates the polarization resistance is relatively small. When the diameter of the semicircle is large as in the case of graphene, the charge transfer resistance is high.

Yang et al. [79] in 2014 showed Nyquist plot of sponge-templated graphene sheets (STGSs) displays a straight line which indicates a behavior characteristic of capacitive nature at the lower frequency region, which is attributed because of fast and easy diffusion of salt ions into

the 3D macropores. But in case of GNs an inclined line as compared with STGS, implies poor diffusion behavior of the ions. The intersecting point in the real axis (X-axis) of the Nyquist plots is referred to the value of the ESR, which includes the electrolyte resistance, electrical resistance between the current collector and the electrode material and the internal electrode. The ESR values obtained for STGS and for GN are 0.84 and 1.16 Ω, respectively. The ESR for STGS was quite small and is because of sufficient exfoliation due to sponge-templated strategy, indicating low internal resistance and fast charge/discharge rate which is appropriate for CDI application. Ahmed G. El-Deen et al. [124] in 2016 found that the carboxylic group (COO^{2-}) rich 3D-activated porous graphene electrode (QC-3DAPGr) cell at high frequency (i.e., left side) shows lower intercepts with the X-axis and small semicircle diameter, indicating small intrinsic resistance of electrodes and low charge transfer resistance compared with all cell configurations. Hence, the asymmetric QC-3DAPGr electrode provides ideal capacitive behavior and lower internal resistances that can improve the desalination performance for CDI.

7.9 Energy Consumption of CDI in Comparison to RO

The current methods of desalinations are RO, electrodialysis, thermal evaporation, and CDI. Among these, RO is most popular, around 85% of desalination plants are based on this technique [125]. RO works on the principle to remove water from the dissolved solids using external pressure, whereas CDI removes ions producing clean water. The typical TDS in sea water is around 35,000 and 1000–4000 ppm for brackish water. Irrespective of the process, the minimum energy required (thermodynamically) for desalinating sea water and brackish water can be calculated theoretically. The minimum energy required for removing ions from a solution are 1.1 and 0.12 kWh/m^3, respectively, for sea water and brackish water. In case of RO, the value depends on the input-output TDS concentration and water recovery [126]. If the ratio is 0.5 the minimum energy required will be 1.6 and 0.17 kWh/m^3, respectively, and energy consumption increases to 2.0 and 0.21, respectively, if the ratio increases to 0.7. Zhao et al. listed out working RO plants in different parts of the world and seen that majority of the RO systems consumes energy around 2 kWh/m^3 with feed concentration below 3.5 g/L. If the feed concentration increases to 8 g/L, the energy consumption increases to 6.5 kWh/m^3 as listed for a RO plant in Lipari, Italy [127]. Besides energy requirement, the final cost of water depends on the size of the unit, operation, and maintenance. A smaller unit having a capacity to produce 1 million gallon of water per day (1 MGD), costs 1.3 \$/m^3, whereas, a bigger unit of 10 MGD able to deliver water for 0.4 \$/m^3 [128]. Major operational cost related to RO is the replacement of the membranes too often.

As discussed earlier, CDI electroadsorb ions from the solution in the double layer formed at the electrodes when a potential difference is applied. For a parallel plate capacitor, the charge separation is electrostatic and depends on area of the plates and the distance of the separation as per the following equation:

$$C = \in_0 \in_r \frac{A}{d} \tag{7.9}$$

where C is the capacitance in F, $\in_0$ is the permittivity of free space (8.854×10^{-12} F/m), $\in_r$ is the relative permittivity of the material between two plates, A is the area of each plates, and d is the distance of separation between the plates (in m).

The capacitors can be connected either parallel or in series and the equivalent capacitance (C_{eq}) can be calculated by the following equations:

$$\text{Parallel}: \quad C_{eq} = \sum C_n \tag{7.10}$$

$$\text{Series}: \quad \left(\frac{1}{C_{eq}}\right) = \sum \frac{1}{C_n} \tag{7.11}$$

Therefore, the energy stored can be calculated as

$$E_{stored} = \frac{1}{2} C V^2 \tag{7.12}$$

where E is the energy (in J), C is the capacitance (in F), and V is the potential difference (in V).

Electrochemically, the capacitance can be calculated using cyclic voltammetry. The operational value is constrained to 1.2–1.5 V because of the redox potential of the water. Considering no Faradic reaction occurs, the capacitance can be directly calculated from the voltammogram and the sweep rate as per the following equation:

$$C = \int \frac{dq}{dV} = I \cdot \int \frac{dt}{dV} = \frac{I}{v} \tag{7.13}$$

where q is the charge (in C), V is the potential difference (in V), I is the current intensity (in A), and v is the sweep rate (V/s).

In case of CDI, as the energy can be easily recovered during the regeneration step. Thus, the net energy required is the difference between the charging (i.e., the adsorption step) and the discharging (i.e., the desorption step)

$$W_{CDI} = W_{charging} - W_{discharging} \tag{7.14}$$

The energy recovered during the discharging step makes the system more energetically favorable that other techniques. Still, much work is needed to develop in electronics and electrochemical methods to efficiently extract the regeneration energy. Since, this strategy can decrease the overall energy requirement of the system, it will be an essential and important part of CDI system in near future. Biesheuvel in 2009 gives a model for calculating maximum theoretical round-trip efficiency for CDI, which was 96% in the case [129]. The efficiency was independent of salt concentration and the regeneration cycle uses only 25% of water as that of

the adsorption cycle. Similarly, Anderson et al. in 2010 theoretically calculated the round-trip efficiency of CDI to produce 1 m^3 of 300 mg/L of clean water from varying concentration (0.5–3.5 g/L) at 1.2 V was 70%–95%.

In the experiments of Farmar et al. in the 1990s, the energy consumption was 0.1 kWh/m^3 to desalinate brackish water. For brackish water (TDS less than 2000 mg/L), CDI requires much less energy than that of RO even with a moderate efficiency of 60%–70% as reported by Zhao et al. [127] If the efficiency of 85% can be attend then CDI will be much energy efficient than that of RO, not only for brackish water but also for sea water as well. Miller and Burke had reported that the round-trip efficiency for carbon-based super capacitor can be as high as 95% in cases [130].

7.10 CDI Technology in Market

The first recognized CDI company to be established was Voltea in 2008, situated in the United States and the Netherlands. They developed a tuneable water desalination technique using MCDI and named it as "CAPDI." They have claimed that the water recovery rate was 95% and it lowers the waste water production by 60% as compared with other membrane-based technologies. They have different products ranging from industrial scale (Fig. 7.14) to a miniature version for domestic use named "DIUSE." From then, different companies have come into existence and the most recognized ones are UR-$WATER_{LLC}$ in the United States

Fig. 7.14
A standard industrial-scale MCDI product developed by Voltea. *Adapted from voltea.com*

formed as a start up with Prof. Anderson, Atlantis Technologies in Canada, Idropan Dell'Orto in Italy, Ionic Engineering Technology Pvt. Ltd. in India, PowerTech Water in the United States and EcoloxTech, which came recently into the CDI market.

Atlantis Technologies claimed that their product removes impurities to 99% and can reduce salinity up to 100,000 ppm with reduced maintenance. Idropan Dell'Orto formed by Tullio Servida have products named Plimmer 4G Alpha and Delta, where they claimed that a TDS of 2000 uS can be reduced to 70%–85% by a single pass and 85%–95% by double pass. They have different partners in countries such as EUROWATER in Denmark, ECOWATER in the United States, AquaSphere in India, and others in Russia, Tunasia, Australia, and Saudi Arabia. PowerTech Water founded in 2014 has just prepared the prototype and is ready for marketing. InnoDI is a new start-up from IIT Madras, established in 2017 and have launched their first domestic CDI product in the market in 2017. Table 7.3 shows a list of CDI companies.

Table 7.3 The leading CDI companies in market in 2018 and their location

Sl. No.	Company	Inventors/MD	Technology	Year of Establish	Location
1	Voltea	Bryan Brister, Jonathan Hodes, Timothy Cavitt	MCDI/CAPDI	2008	Wasbeekerlaan 24, 2171 AE Sassenheim, The Netherlands
2	UR_WATER$_{LLC}$	Mr. John Etter and Prof. Marc Anderson	Modified CDI	~2012	Madison, WI 53718, United States
3	Idropan Dell'Orto	Tullio Servida	MCDI	~2012	Via Valassina 19 20159 Milan, Italy
4	Atlantis Technologies	Patrick Curran, Brian Hill	Radial deionization	~2014	32932, Pacific Coast Hwy #14, Dana Point, CA 92629, United States
5	Current Water Technologies inc.	Dr. Gene S. Shelp	Electro-static deionization	~2016	70 Southgate Drive, Unit 4 Guelph, ON, Canada
6	Ionic Engineering Technology Pvt. Ltd.	K.V. Raman	CAPDI[c]	~2016	Ground Floor, B Wing, Mahalaxmi Heights, Mumbai, India
7	PowerTech Water, LLC	Dr. Cameron Lippert	Inverted-CDI	~2016	Lexington, KY, United States
8	InnoDI (An IITM incubated (company)	Tullio Servida, Vijay Sampath, Prof. T. Pradeep	MCDI	2017	Bangalore, India

7.11 Conclusions

The field of CDI has seen a tremendous growth in the last two decades. It has come out from the laboratories to commercial market as a product for water desalination. Different novel active carbon materials have come out in the last few years with high electroadsorption capacity with different cell architecture. Currently, it is possible to deliver water of any derived quality and quantity with CDI. Even the cost of clean water is comparable to RO. Thermodynamic energy requirement for desalination using capacitive electrodes is much less than the actual energy required. So, there is a scope for further improvement of thermodynamic efficiency in future [5].

Acknowledgments

We acknowledge our colleagues who have contributed for the development of CDI technology in our laboratory. Department of Science and Technology for several grants, Government of India is thanked for the financial support.

References

[1] http://www.un.org/News/Press/docs/2010/ga10967.doc.htm.
[2] Andelman, M.; Walker, G., Charge barrier flow-through capacitor. Google Patents 2004.
[3] S. Porada, R. Zhao, A. van der Wal, V. Presser, P.M. Biesheuvel, Review on the science and technology of water desalination by capacitive deionization, Prog. Mater. Sci. 58 (8) (2013) 1388–1442.
[4] J.-B. Lee, K.-K. Park, H.-M. Eum, C.-W. Lee, Desalination of a thermal power plant wastewater by membrane capacitive deionization, Desalination 196 (1) (2006) 125–134.
[5] P. Długołęcki, A. van der Wal, Energy recovery in membrane capacitive deionization, Environ. Sci. Technol. 47 (9) (2013) 4904–4910.
[6] O.N. Demirer, R.M. Naylor, C.A. Rios Perez, E. Wilkes, C. Hidrovo, Energetic performance optimization of a capacitive deionization system operating with transient cycles and brackish water, Desalination 314 (2013) 130–138.
[7] S. Evans, W. Hamilton, The mechanism of demineralization at carbon electrodes, J. Electrochem. Soc. 113 (12) (1966) 1314–1319.
[8] G.W. Reid, A. Stevens, J. Abichandani, F. Townsend, M. Al-Awady, Field Operation of a 20 Gallons Per Day Pilot Plant Unit for Electrochemical Desalination of Brackish Water, U.S. Dept. of the Interior, Washington, DC, 1968.
[9] J. Newman, R.G. Wilbourne, A.W. Venolia, A.M. Johnson, C. Marquardt, United States, The Electrosorb Process for Desalting Water, U.S. Dept. of the Interior, Washington, DC, 1970, p. iii 31 p.
[10] A.M. Johnson, J. Newman, Desalting by means of porous carbon electrodes, J. Electrochem. Soc. 118 (3) (1971) 510–517.
[11] J.C. Farmer, D.V. Fix, G.V. Mack, R.W. Pekala, J.F. Poco, Capacitive deionization of NaCl and NaNO3 solutions with carbon aerogel electrodes, J. Electrochem. Soc. 143 (1) (1996) 159–169.
[12] (a)Farmer, J., Method and apparatus for capacitive deionization, electrochemical purification, and regeneration of electrodes. Google Patents: 1995;(b)Farmer, J. C., Method and apparatus for capacitive deionization and electrochemical purification and regeneration of electrodes. Google Patents: 1999;(c)Tran, T. D.; Farmer, J. C.; Murguia, L., Method and apparatus for capacitive deionization and electrochemical purification and regeneration of electrodes. Google Patents: 2001.
[13] Suss, M. E.; Baumann, T. F.; Bourcier, W. L.; Spadaccini, C.; Stadermann, M.; Rose, K.; Santiago, J. G., Flow-through electrode capacitive desalination. Google Patents 2012.

[14] T. Welgemoed, C. Schutte, Capacitive deionization technology: an alternative desalination solution, Desalination 183 (1–3) (2005) 327–340.
[15] P. Biesheuvel, A. Van der Wal, Membrane capacitive deionization, J. Membr. Sci. 346 (2) (2010) 256–262.
[16] Y.-J. Kim, J.-H. Choi, Selective removal of nitrate ion using a novel composite carbon electrode in capacitive deionization, Water Res. 46 (18) (2012) 6033–6039.
[17] S.-I. Jeon, H.-R. Park, J.-G. Yeo, S. Yang, C.H. Cho, M.H. Han, D.K. Kim, Desalination via a new membrane capacitive deionization process utilizing flow-electrodes, Energy Environ. Sci. 6 (5) (2013) 1471–1475.
[18] M. Andelman, Ionic group derivitized nano porous carbon electrodes for capacitive deionization, J. Mater. Sci. Chem. Eng. 02 (03) (2014) 7.
[19] Nyberg, E. D., Electrochemically assisted ion exchange. Google Patents 1998.
[20] Andelman, M. D., Energy and weight efficient flow-through capacitor, system and method. Google Patents 2001.
[21] Andelman, M. D., Charge barrier flow-through capacitor. Google Patents 2002.
[22] Inoue, H.; Yamanaka, K.; Tamura, M.; Yoshida, S.; Nakamura, H., Ion exchanger. Google Patents 2003.
[23] Shiue, L. R.; Sun, A.; Shiue, C. C.; Hsieh, F. C.; Hsieh, Y. H.; Jou, J. J., Deionizers with energy recovery. Google Patents 2003.
[24] Yang, H. J.; Kang, H.; Song, T.; Kim, C. H., Electrode for capacitive deionization, capacitive deionization device and electric double layer capacitor including the electrode. Google Patents 2010.
[25] Yang, H. J.; Kang, H.; KIM, K.; KIM, J., Transition metal/carbon nanotube composite and method of preparing the same. Google Patents 2010.
[26] Yang, H. J.; Kang, H.; Song, T.; Kim, C. H., Integrated electrode-current collector sheet for capacitive deionization, capacitive deionization device and electric double layer capacitor having the same. Google Patents 2013.
[27] Altaee, A., Capacitive deionization. Google Patents 2010.
[28] KNAPP, S.; Leffew, M., Method of regenerating a capacitive deionization cell. Google Patents 2010.
[29] Kang, K. S.; Choi, J. H., Capacitive electrode for deionization, and electrolytic cell using same. Google Patents 2012.
[30] Kim, C. H.; Kang, H.; Yang, H. J.; Kim, H., Capacitive deionization device. Google Patents 2011.
[31] Kang, K. S.; Son, W. K.; Choi, J. H.; Park, N. S.; Kim, T. I., Ion-selective capacitive deionization composite electrode, and method for manufacturing a module. Google Patents 2012.
[32] Ramaprabhu, S.; Mishra, A. K., Methods and systems for separating ions from fluids. Google Patents 2012.
[33] Averbeck, D. J.; Tallon, R. M.; Boedeker, B. A., Ion removal using a capacitive deionization system. Google Patents 2017.
[34] Averbeck, D. J.; Tallon, R. M.; Boedeker, B. A., Regeneration of a capacitive deionization system. Google Patents 2017.
[35] Sun, Z.; Pan, L.; Li, H.; Sun, Y., Membrane enhanced deionization capacitor device. Google Patents 2013.
[36] Andelman, M. D., Polarized electrode for flow-through capacitive deionization. Google Patents 2012.
[37] Jung, M. I. I.; Ko, Y. C.; JEONG, I. J.; Mingming, Y.; Yeo, H. S., Capacitive deionization apparatus. Google Patents 2013.
[38] Jeong, J. S.; Kim, H. S.; PARK, D. H.; Ham, D. J.; Kang, H. R., Capacitive deionization apparatus and methods of treating fluid using the same. Google Patents 2014.
[39] Kang, K. S.; Son, W. K.; Kim, T. I.; Kim, M. Y., Method of manufacturing capacitive deionization electrode having ion selectivity and CDI electrode module including the same. Google Patents 2013.
[40] ABRAMI, A.; TAMBURINI, F., Method and plant for the reduction of the concentration of pollutants and/or valuable elements in the water. Google Patents 2014.
[41] Simon, P.; Taberna, P. L.; Daffos, B.; Iwama, E.; Tzedakis, T.; Gogotsi, Y.; Hatzell, K.; Gogotsi, O., Method and device to remove ions from an electrolytic media, such as water desalination, using suspension of divided materials in a flow capacitor. Google Patents 2014.
[42] Cho, M. D.; Kim, H. S.; JEONG, J. S., Composition for electrode of capacitive deionization apparatus, and electrode including same. Google Patents 2017.
[43] Yang, Y. S.; Kim, J. E.; Kim, H. S.; Lee, S. J.; Kang, H. R.; JEONG, J. S., Capacitive deionization electrodes, capacitive deionization apparatuses including the same, and production methods thereof. Google Patents 2017.

[44] Jeong, J. S.; Kim, H. S.; Cho, M. D.; Kang, H. R., Regeneration methods of capacitive deionization electrodes. Google Patents 2015.
[45] Choi, Y. S.; Lee, S. J.; Jeong, J. S., Composition for electrode of capacitive deionization apparatus, and electrode including same. Google Patents 2015.
[46] Cai, Z.; Schwannecke, J. K.; Anderson, D. J.; Taylor, R. M., Capacitive deionization system, electrode pack and method for operating the system. Google Patents 2015.
[47] Atieh, M. A.; Laoui, T., Fabrication of carbon nanotube membranes. Google Patents 2017.
[48] Liu, P. I.; Chung, L. C.; Liang, T. M.; Horng, R. Y.; Shao, H.; Chen, R. S.; Fan, H. T.; Fang, C. H.; Chang, M. C., Binder for capacitive deionization electrode and method for manufacturing the same. Google Patents 2017.
[49] Choi, Y.; Lim, J. W., Electrode composition for capacitive deionization device, and electrode for capacitive deionization device containing the same. Google Patents 2017.
[50] Choi, H. S.; Choi, S. H.; Hwang, S. H.; Choi, W.; Kim, S., Capacitive deionization apparatus. Google Patents 2017.
[51] DANIEL, J.; Ghosh, S.; Rajanarayana, V., Electrode for capacitive deionization. Google Patents 2017.
[52] Ryu, T. G.; Kim, B. G.; Ryu, J. H.; Park, I. S.; Hong, H. J.; Chung, K. S., System for recovering multiple kinds of ions. Google Patents 2017.
[53] F.A. AlMarzooqi, A.A. Al Ghaferi, I. Saadat, N. Hilal, Application of capacitive deionisation in water desalination: a review, Desalination 342 (2014) 3–15.
[54] H. Helmholtz, Helmholtz's theory of double electric layers, J. Frankl. Inst. 115 (4) (1883) 310.
[55] E. Avraham, M. Noked, Y. Bouhadana, A. Soffer, D. Aurbach, Limitations of charge efficiency in capacitive deionization II. On the behavior of CDI cells comprising two activated carbon electrodes, J. Electrochem. Soc. 156 (10) (2009) 157–162.
[56] Y.-J. Kim, J.-H. Choi, Improvement of desalination efficiency in capacitive deionization using a carbon electrode coated with an ion-exchange polymer, Water Res. 44 (3) (2010) 990–996.
[57] (a) R. Zhao, P.M. Biesheuvel, A. van der Wal, Energy consumption and constant current operation in membrane capacitive deionization, Energy Environ. Sci. 5 (11) (2012) 9520–9527; (b) P. Biesheuvel, R. Zhao, S. Porada, A. Van der Wal, Theory of membrane capacitive deionization including the effect of the electrode pore space, J. Colloid Interface Sci. 360 (1) (2011) 239–248.
[58] A. Soffer, M. Folman, The electrical double layer of high surface porous carbon electrode, J. Electroanal. Chem. Interfacial Electrochem. 38 (1) (1972) 25–43.
[59] K.-L. Yang, T.-Y. Ying, S. Yiacoumi, C. Tsouris, E.S. Vittoratos, Electrosorption of ions from aqueous solutions by carbon aerogel: an electrical double-layer model, Langmuir 17 (6) (2001) 1961–1969.
[60] K. Dai, L. Shi, J. Fang, D. Zhang, B. Yu, NaCl adsorption in multi-walled carbon nanotubes, Mater. Lett. 59 (16) (2005) 1989–1992.
[61] S. Wang, D. Wang, L. Ji, Q. Gong, Y. Zhu, J. Liang, Equilibrium and kinetic studies on the removal of NaCl from aqueous solutions by electrosorption on carbon nanotube electrodes, Sep. Purif. Technol. 58 (1) (2007) 12–16.
[62] P. Xu, J.E. Drewes, D. Heil, G. Wang, Treatment of brackish produced water using carbon aerogel-based capacitive deionization technology, Water Res. 42 (10) (2008) 2605–2617.
[63] H. Li, T. Lu, L. Pan, Y. Zhang, Z. Sun, Electrosorption behavior of graphene in NaCl solutions, J. Mater. Chem. 19 (37) (2009) 6773–6779.
[64] H. Li, L. Zou, L. Pan, Z. Sun, Novel graphene-like electrodes for capacitive deionization, Environ. Sci. Technol. 44 (22) (2010) 8692–8697.
[65] R. Zhao, P.M. Biesheuvel, H. Miedema, H. Bruning, A. van der Wal, Charge efficiency: a functional tool to probe the double-layer structure inside of porous electrodes and application in the modeling of capacitive deionization, J. Phys. Chem. Lett. 1 (1) (2010) 205–210.
[66] C. Tsouris, R. Mayes, J. Kiggans, K. Sharma, S. Yiacoumi, D. DePaoli, S. Dai, Mesoporous carbon for capacitive deionization of saline water, Environ. Sci. Technol. 45 (23) (2011) 10243–10249.
[67] J. Landon, X. Gao, B. Kulengowski, J.K. Neathery, K. Liu, Impact of pore size characteristics on the electrosorption capacity of carbon xerogel electrodes for capacitive deionization, J. Electrochem. Soc. 159 (11) (2012) A1861–A1866.

[68] H. Wang, D. Zhang, T. Yan, X. Wen, L. Shi, J. Zhang, Graphene prepared via a novel pyridine–thermal strategy for capacitive deionization, J. Mater. Chem. 22 (45) (2012) 23745–23748.
[69] Z. Wang, B. Dou, L. Zheng, G. Zhang, Z. Liu, Z. Hao, Effective desalination by capacitive deionization with functional graphene nanocomposite as novel electrode material, Desalination 299 (2012) 96–102.
[70] B. Jia, L. Zou, Graphene nanosheets reduced by a multi-step process as high-performance electrode material for capacitive deionisation, Carbon 50 (6) (2012) 2315–2321.
[71] M.E. Suss, T.F. Baumann, W.L. Bourcier, C.M. Spadaccini, K.A. Rose, J.G. Santiago, M. Stadermann, Capacitive desalination with flow-through electrodes, Energy Environ. Sci. 5 (11) (2012) 9511–9519.
[72] D. Zhang, X. Wen, L. Shi, T. Yan, J. Zhang, Enhanced capacitive deionization of graphene/mesoporous carbon composites, Nanoscale 4 (17) (2012) 5440–5446.
[73] D. Zhang, T. Yan, L. Shi, Z. Peng, X. Wen, J. Zhang, Enhanced capacitive deionization performance of graphene/carbon nanotube composites, J. Mater. Chem. 22 (29) (2012) 14696–14704.
[74] H. Li, L. Pan, C. Nie, Y. Liu, Z. Sun, Reduced graphene oxide and activated carbon composites for capacitive deionization, J. Mater. Chem. 22 (31) (2012) 15556–15561.
[75] Z. Peng, D. Zhang, L. Shi, T. Yan, High performance ordered mesoporous carbon/carbon nanotube composite electrodes for capacitive deionization, J. Mater. Chem. 22 (14) (2012) 6603–6612.
[76] X. Wen, D. Zhang, T. Yan, J. Zhang, L. Shi, Three-dimensional graphene-based hierarchically porous carbon composites prepared by a dual-template strategy for capacitive deionization, J. Mater. Chem. A 1 (39) (2013) 12334–12344.
[77] G. Wang, B. Qian, Q. Dong, J. Yang, Z. Zhao, J. Qiu, Highly mesoporous activated carbon electrode for capacitive deionization, Sep. Purif. Technol. 103 (2013) 216–221.
[78] H. Yin, S. Zhao, J. Wan, H. Tang, L. Chang, L. He, H. Zhao, Y. Gao, Z. Tang, Three-dimensional graphene/metal oxide nanoparticle hybrids for high-performance capacitive deionization of saline water, Adv. Mater. 25 (43) (2013) 6270–6276.
[79] Z.Y. Yang, L.J. Jin, G.Q. Lu, Q.Q. Xiao, Y.X. Zhang, L. Jing, X.X. Zhang, Y.M. Yan, K.N. Sun, Sponge-templated preparation of high surface area graphene with ultrahigh capacitive deionization performance, Adv. Funct. Mater. 24 (25) (2014) 3917–3925.
[80] Y. Liu, L. Pan, X. Xu, T. Lu, Z. Sun, D.H. Chua, Carbon nanorods derived from natural based nanocrystalline cellulose for highly efficient capacitive deionization, J. Mater. Chem. A 2 (48) (2014) 20966–20972.
[81] A.G. El-Deen, N.A.M. Barakat, H.Y. Kim, Graphene wrapped MnO2-nanostructures as effective and stable electrode materials for capacitive deionization desalination technology, Desalination 344 (2014) 289–298.
[82] X. Xu, L. Pan, Y. Liu, T. Lu, Z. Sun, D.H. Chua, Facile synthesis of novel graphene sponge for high performance capacitive deionization, Sci. Rep. (5) (2015). srep08458.
[83] N. Pugazhenthiran, S. Sen Gupta, A. Prabhath, M. Manikandan, J.R. Swathy, V.K. Raman, T. Pradeep, Cellulose derived graphenic fibers for capacitive desalination of brackish water, ACS Appl. Mater. Interfaces 7 (36) (2015) 20156–20163.
[84] A.G. El-Deen, J.-H. Choi, C.S. Kim, K.A. Khalil, A.A. Almajid, N.A. Barakat, TiO 2 nanorod-intercalated reduced graphene oxide as high performance electrode material for membrane capacitive deionization, Desalination 361 (2015) 53–64.
[85] G. Rasines, P. Lavela, C. Macías, M.C. Zafra, J.L. Tirado, J.B. Parra, C.O. Ania, N-doped monolithic carbon aerogel electrodes with optimized features for the electrosorption of ions, Carbon 83 (2015) 262–274.
[86] X. Xu, Y. Liu, T. Lu, Z. Sun, D.H. Chua, L. Pan, Rational design and fabrication of graphene/carbon nanotubes hybrid sponge for high-performance capacitive deionization, J. Mater. Chem. A 3 (25) (2015) 13418–13425.
[87] R. Kumar, S.S. Gupta, S. Katiyar, V.K. Raman, S.K. Varigala, T. Pradeep, A. Sharma, Carbon aerogels through organo-inorganic co-assembly and their application in water desalination by capacitive deionization, Carbon 99 (2016) 375–383.
[88] A.S. Yasin, H.O. Mohamed, I.M. Mohamed, H.M. Mousa, N.A. Barakat, Enhanced desalination performance of capacitive deionization using zirconium oxide nanoparticles-doped graphene oxide as a novel and effective electrode, Sep. Purif. Technol. 171 (2016) 34–43.
[89] H. Zhang, P. Liang, Y. Bian, Y. Jiang, X. Sun, C. Zhang, X. Huang, F. Wei, Moderately oxidized graphene–carbon nanotubes hybrid for high performance capacitive deionization, RSC Adv. 6 (64) (2016) 58907–58915.

[90] S. Zhao, T. Yan, H. Wang, G. Chen, L. Huang, J. Zhang, L. Shi, D. Zhang, High capacity and high rate capability of nitrogen-doped porous hollow carbon spheres for capacitive deionization, Appl. Surf. Sci. 369 (2016) 460–469.
[91] W. Kong, X. Duan, Y. Ge, H. Liu, J. Hu, X. Duan, Holey graphene hydrogel with in-plane pores for high-performance capacitive desalination, Nano Res. 9 (8) (2016) 2458–2466.
[92] X. Xu, M. Wang, Y. Liu, T. Lu, L. Pan, Metal–organic framework-engaged formation of a hierarchical hybrid with carbon nanotube inserted porous carbon polyhedra for highly efficient capacitive deionization, J. Mater. Chem. A 4 (15) (2016) 5467–5473.
[93] T. Gao, H. Li, F. Zhou, M. Gao, S. Liang, M. Luo, Mesoporous carbon derived from ZIF-8 for high efficient electrosorption, Desalination (2017).
[94] D. Xu, Y. Tong, T. Yan, L. Shi, D. Zhang, N, P-co-doped meso-/microporous carbon derived from biomass materials via a dual-activation strategy as high-performance electrodes for deionization capacitors, ACS Sustain. Chem. Eng. (2017).
[95] S. Zhao, T. Yan, Z. Wang, J. Zhang, L. Shi, D. Zhang, Removal of NaCl from saltwater solutions using micro/mesoporous carbon sheets derived from watermelon peel via deionization capacitors, RSC Adv. 7 (8) (2017) 4297–4305.
[96] H. Wang, T. Yan, L. Shi, G. Chen, J. Zhang, D. Zhang, Creating nitrogen-doped hollow multiyolk@ shell carbon as high performance electrodes for flow-through deionization capacitors, ACS Sustain. Chem. Eng. 5 (4) (2017) 3329–3338.
[97] T. Wu, G. Wang, Q. Dong, F. Zhan, X. Zhang, S. Li, H. Qiao, J. Qiu, Starch derived porous carbon nanosheets for high-performance photovoltaic capacitive deionization, Environ. Sci. Technol. 51 (16) (2017) 9244–9251.
[98] K.S.W. Sing, D.H. Everett, R.A.W. Haul, L. Moscou, R.A. Pierotti, J. Rouquerol, T. Siemieniewska, Reporting physisorption data for gas/solid systems, in: G. Ertl, H. Knözinger, F. Schüth, J. Weitkamp (Eds.), Handbook of Heterogeneous Catalysis, Wiley Online Library, 2008, https://doi.org/10.1002/9783527610044.hetcat0065.
[99] H. Shi, Activated carbons and double layer capacitance, Electrochim. Acta 41 (10) (1996) 1633–1639.
[100] Y. Marcus, Thermodynamics of solvation of ions. Part 5.—Gibbs free energy of hydration at 298.15 K, J. Chem. Soc. Faraday Trans. 87 (18) (1991) 2995–2999.
[101] J. Gamby, P.L. Taberna, P. Simon, J.F. Fauvarque, M. Chesneau, Studies and characterisations of various activated carbons used for carbon/carbon supercapacitors, J. Power Sources 101 (1) (2001) 109–116.
[102] L. Zou, G. Morris, D. Qi, Using activated carbon electrode in electrosorptive deionisation of brackish water, Desalination 225 (1-3) (2008) 329–340.
[103] A. Zeng, M. Shrestha, K. Wang, V.F. Neto, B. Gabriel, Q.H. Fan, Plasma treated active carbon for capacitive deionization of saline water, J. Nanomater. 2017 (2017) 8.
[104] J.J. Lado, R.L. Zornitta, F.A. Calvi, M. Martins, M.A. Anderson, F.G.E. Nogueira, L.A.M. Ruotolo, Enhanced capacitive deionization desalination provided by chemical activation of sugar cane bagasse fly ash electrodes, J. Anal. Appl. Pyrolysis *126* (Suppl. C) (2017) 143–153.
[105] T. Alencherry, A. Naveen, S. Ghosh, J. Daniel, R. Venkataraghavan, Effect of increasing electrical conductivity and hydrophilicity on the electrosorption capacity of activated carbon electrodes for capacitive deionization, Desalination 415 (2017) 14–19.
[106] P.A. Chen, H.C. Cheng, H.P. Wang, Activated carbon recycled from bitter-tea and palm shell wastes for capacitive desalination of salt water, J. Clean. Prod. *174* (Suppl. C) (2018) 927–932.
[107] A.S. Yasin, I.M. Mohamed, H.M. Mousa, C.H. Park, C.S. Kim, Facile synthesis of TiO 2/ZrO 2 nanofibers/nitrogen co-doped activated carbon to enhance the desalination and bacterial inactivation via capacitive deionization, Sci. Rep. 8 (1) (2018) 541.
[108] L. Zou, L. Li, H. Song, G. Morris, Using mesoporous carbon electrodes for brackish water desalination, Water Res. 42 (8) (2008) 2340–2348.
[109] L. Li, L. Zou, H. Song, G. Morris, Ordered mesoporous carbons synthesized by a modified sol–gel process for electrosorptive removal of sodium chloride, Carbon 47 (3) (2009) 775–781.
[110] R.W. Pekala, C.T. Alviso, F.M. Kong, S.S. Hulsey, Aerogels derived from multifunctional organic monomers, J. Non-Cryst. Solids 145 (1992) 90–98.

[111] H.-H. Jung, S.-W. Hwang, S.-H. Hyun, K.-H. Lee, G.-T. Kim, Capacitive deionization characteristics of nanostructured carbon aerogel electrodes synthesized via ambient drying, Desalination 216 (1-3) (2007) 377–385.
[112] S. Porada, L. Weinstein, R. Dash, A. van der Wal, M. Bryjak, Y. Gogotsi, P.M. Biesheuvel, Water desalination using capacitive deionization with microporous carbon electrodes, ACS Appl. Mater. Interfaces 4 (3) (2012) 1194–1199.
[113] R.H. Baughman, A.A. Zakhidov, W.A. De Heer, Carbon nanotubes—the route toward applications, S*cience 297* (5582) (2002) 787–792.
[114] C. Yan, L. Zou, R. Short, Single-walled carbon nanotubes and polyaniline composites for capacitive deionization, Desalination 290 (2012) 125–129.
[115] L. Wang, M. Wang, Z.-H. Huang, T. Cui, X. Gui, F. Kang, K. Wang, D. Wu, Capacitive deionization of NaCl solutions using carbon nanotube sponge electrodes, J. Mater. Chem. 21 (45) (2011) 18295–18299.
[116] M. Moronshing, C. Subramaniam, Scalable approach to highly efficient and rapid capacitive deionization with CNT-thread as electrodes, ACS Appl. Mater. Interfaces 9 (46) (2017) 39907–39915.
[117] K.S. Novoselov, A.K. Geim, S.V. Morozov, D. Jiang, Y. Zhang, S.V. Dubonos, I.V. Grigorieva, A.A. Firsov, Electric field effect in atomically thin carbon films, Science *306* (5696) (2004) 666–669.
[118] H. Li, L. Zou, L. Pan, Z. Sun, Using graphene nano-flakes as electrodes to remove ferric ions by capacitive deionization, Sep. Purif. Technol. 75 (1) (2010) 8–14.
[119] H. Wang, D. Zhang, T. Yan, X. Wen, J. Zhang, L. Shi, Q. Zhong, Three-dimensional macroporous graphene architectures as high performance electrodes for capacitive deionization, J. Mater. Chem. A 1 (38) (2013) 11778–11789.
[120] G. Luo, Y. Wang, L. Gao, D. Zhang, T. Lin, Graphene bonded carbon nanofiber aerogels with high capacitive deionization capability, Electrochim. Acta 260 (2018) 656–663.
[121] J. Li, B. Ji, R. Jiang, P. Zhang, N. Chen, G. Zhang, L. Qu, Hierarchical hole-enhanced 3D graphene assembly for highly efficient capacitive deionization, Carbon 129 (2018) 95–103.
[122] F. Meng, Q. Zhao, X. Na, Z. Zheng, J. Jiang, L. Wei, J. Zhang, Bioelectricity generation and dewatered sludge degradation in microbial capacitive desalination cell, Environ. Sci. Pollut. Res. 24 (6) (2017) 5159–5167.
[123] H. Li, S. Liang, J. Li, L. He, The capacitive deionization behaviour of a carbon nanotube and reduced graphene oxide composite, J. Mater. Chem. A 1 (21) (2013) 6335–6341.
[124] A.G. El-Deen, R.M. Boom, H.Y. Kim, H. Duan, M.B. Chan-Park, J.-H. Choi, Flexible 3D nanoporous graphene for desalination and bio-decontamination of brackish water via asymmetric capacitive deionization, ACS Appl. Mater. Interfaces 8 (38) (2016) 25313–25325.
[125] R. Borsani, S. Rebagliati, Fundamentals and costing of MSF desalination plants and comparison with other technologies, Desalination 182 (1) (2005) 29–37.
[126] M.A. Anderson, A.L. Cudero, J. Palma, Capacitive deionization as an electrochemical means of saving energy and delivering clean water. Comparison to present desalination practices: will it compete? Electrochim. Acta 55 (12) (2010) 3845–3856.
[127] R. Zhao, S. Porada, P.M. Biesheuvel, A. van der Wal, Energy consumption in membrane capacitive deionization for different water recoveries and flow rates, and comparison with reverse osmosis, Desalination 330 (2013) 35–41.
[128] I.C. Karagiannis, P.G. Soldatos, Water desalination cost literature: review and assessment, Desalination 223 (1-3) (2008) 448–456.
[129] P. Biesheuvel, Thermodynamic cycle analysis for capacitive deionization, J. Colloid Interface Sci. 332 (1) (2009) 258–264.
[130] J.R. Miller, A.F. Burke, Electrochemical capacitors: challenges and opportunities for real-world applications, Electrochem. Soc. Interface 17 (1) (2008) 53.